GROUNDWATER MODEL OF THE WEST CRANE AQUIFER, RICHLAND COUNTY, MONTANA

Kurt Zeiler, Kevin Chandler, and Jon Reiten
Ground Water Investigation Program

MBMG
Montana Bureau of Mines and Geology

Front photo: Irrigation well in the West Crane aquifer, with low rolling hills of glacial deposits in the background on the right and Cretaceous Fort Union Formation in the distant background on the left. Photo by Jon Reiten.

GROUNDWATER MODEL OF THE WEST CRANE AQUIFER, RICHLAND COUNTY, MONTANA

Kurt Zeiler, Kevin Chandler, and Jon Reiten

Montana Bureau of Mines and Geology Open-File Report 774

June 2025

https://doi.org/10.59691/EBTP2447

TABLE OF CONTENTS

FIGURES

TABLES

PREFACE

The Montana Bureau of Mines and Geology (MBMG) Ground Water Investigation Program (GWIP) investigates areas prioritized by the Ground Water Assessment Steering Committee (2-15-1523 MCA) based on current and anticipated growth of industry, housing and commercial activity, or agriculture. Additional program information and project ranking details are available at http://www.mbmg.mtech.edu/ (Ground Water Investigation Program).

The final products of the GWIP's West Crane aquifer study include:

- An **Information Pamphlet** (Chandler and Reiten, 2020) that provides a basic description of the aquifer, its general groundwater flow conditions, monitoring activities, and future planning considerations.
- An **Aquifer Test Summary Report** (Reiten and Chandler, 2021) that describes aquifer tests and results for the West Crane aquifer.
- A **Hydrogeologic Report** (Reiten and Chandler, 2023) that presents data, interpretations, and summarizes the project results. The focus of this report is on defining the extent and hydrogeology of the West Crane aquifer and addressing potential changes to surface water and groundwater from increased irrigation development of the West Crane aquifer.
- A **Groundwater Modeling Report** (this report) that documents development of a groundwater flow model with steady-state and transient versions, including a detailed description of the procedures, assumptions, and results of the models. Groundwater modelers and other qualified individuals can evaluate and use the models as a starting point to test additional water use scenarios and for site-specific analyses.

MBMG's Groundwater Information Center (GWIC) online database (http://mbmggwic.mtech.edu/) provides a permanent archive for the data from this study.

ABSTRACT

The West Crane aquifer underlies the western slopes of the Yellowstone River valley between Fox Creek (north) and Burns Creek (south) in Richland County, Montana. The aquifer occupies a buried valley eroded into the Fort Union Formation that runs parallel to the Yellowstone River valley. Test drilling performed between 2012 and 2018 revealed a sinuous buried valley that is about 1 mi wide, up to 300 ft deep, with a gradient similar to the modern Yellowstone River.

Seven west-to-east drainages cross the buried valley, forming dry washes above the aquifer. These ephemeral drainages are often flowing where the streams have eroded into the Fort Union Formation bedrock along the eastern edge of the aquifer. The gravel at the base of the buried valley is the most productive sediment in the buried valley aquifer, supporting well yields up to 1,300 gpm. The overlying leaky confining unit provides a large volume of storage, which helps to maintain aquifer head.

As of 2020, 14 irrigation wells were completed in the West Crane aquifer. Eleven of these were drilled since 2009. Aquifer tests conducted at each irrigation well have provided information regarding the hydraulic conductivity and storativity of the aquifer. The potential for increased irrigation withdrawals from the aquifer prompted the Richland County Conservation District to propose this Montana Bureau of Mines and Geology's Ground Water Investigation Program project with goals to determine the aquifer extent, hydraulic characteristics, and water quality, and to model the aquifer flow system.

A groundwater flow model with steady-state and 1-year transient versions was developed to simulate the aquifer response to three scenarios: no-pumping, pumping (at 2019 volumes), and increased pumping (maximum allocation volume). These scenarios show that groundwater withdrawals from the buried valley aquifer, tend to be primarily balanced by changes in the amounts of water entering and/or retrieved from storage. Pumping the irrigation wells at their full allocated volumes resulted in approximately 14 percent decreased discharge to streams when compared to the 2019 baseline model. A managed aquifer recharge scenario that simulated infiltration of water into gravel pits, increased groundwater storage by about 58 percent compared to the baseline model, though approximately 27 percent of the recharged water was simulated to discharge to surface water downstream. The groundwater models developed as-is, or modified with new data, will be an important tool for water managers to address ongoing irrigation development of the West Crane aquifer.

INTRODUCTION

The West Crane buried valley aquifer spans 22 mi between Burns Creek and Fox Creek, paralleling the modern Yellowstone River (fig. 1; Chandler and Reiten, 2020). The aquifer is connected to the Sidney aquifer to the north, which continues on into North Dakota at Fairview. The West Crane aquifer supports high-yield irrigation wells (300–1,300 gpm) in an area that was historically dry-land farming and pasture. The rise in demand for irrigation water and the increasing development of this aquifer prompted the Richland County Conservation District to propose this Ground Water Investigation Program (GWIP) project and groundwater flow model development. Farmers and water managers want to know the potential of the aquifer and how new irrigation development will affect existing irrigation systems and the streams discharging from the aquifer.

Objectives

The objective of the study was to evaluate the extent and groundwater availability of the West Crane aquifer. This report describes the numerical groundwater flow model that was used to refine a groundwater budget, and to evaluate changes in the aquifer system in response to ongoing development. Three hypothetical scenarios were evaluated regarding the timing and increase in water use for irrigation. A fourth scenario evaluated the effects of managed aquifer recharge (MAR) by infiltrating water into gravel pits as a means of increasing groundwater recharge and aquifer storage.

The West Crane groundwater model was initially built using Groundwater Modeling System (GMS) software (Aquaveo, 2009, 2019) with MODFLOW-2000 (Harbaugh and others, 2000) and MODFLOW-2005 (Harbaugh, 2005). The final model construction used Groundwater Vistas version 8 (ESI, 2020) with MODFLOW 6 (Langevin and others, 2017). This report provides the details on model construction, operation, calibration, and sensitivity analysis. The final MODFLOW 6 input files are provided in plain-text formats that can then be imported to any pre-/post-processing software that supports MODFLOW 6.

The steady-state model version is based on March 2018 information, and the transient 1-yr model version was developed for 2019. Hydraulic conductivity, drain conductance, and recharge input values were initially developed using parameter estimation (PEST) with the steady-state model version. The final PEST calibration process was performed for hydraulic conductivity (horizontal and vertical) and storage parameter input values on both the steady-state and 1-yr transient model versions together to retain consistent input values between both versions.

Model Area

The model area extends the length (22 mi) and width (about 1 mi) of the aquifer, covering approximately 45.8 mi^2. The model boundary was set slightly wider than the aquifer to include Fort Union bedrock that bounds the aquifer on the east and west and provides some lateral inter-aquifer flow to the buried valley (fig. 1).

Area Description

The West Crane aquifer is part of the Lower Yellowstone buried valley aquifer (LYBV). The LYBV can be divided into three aquifers (fig. 1; Chandler and Reiten, 2020). The northern part of the aquifer (the Sidney aquifer) extends from near Fairview to Fox Creek and is recharged by deep percolation of irriga-

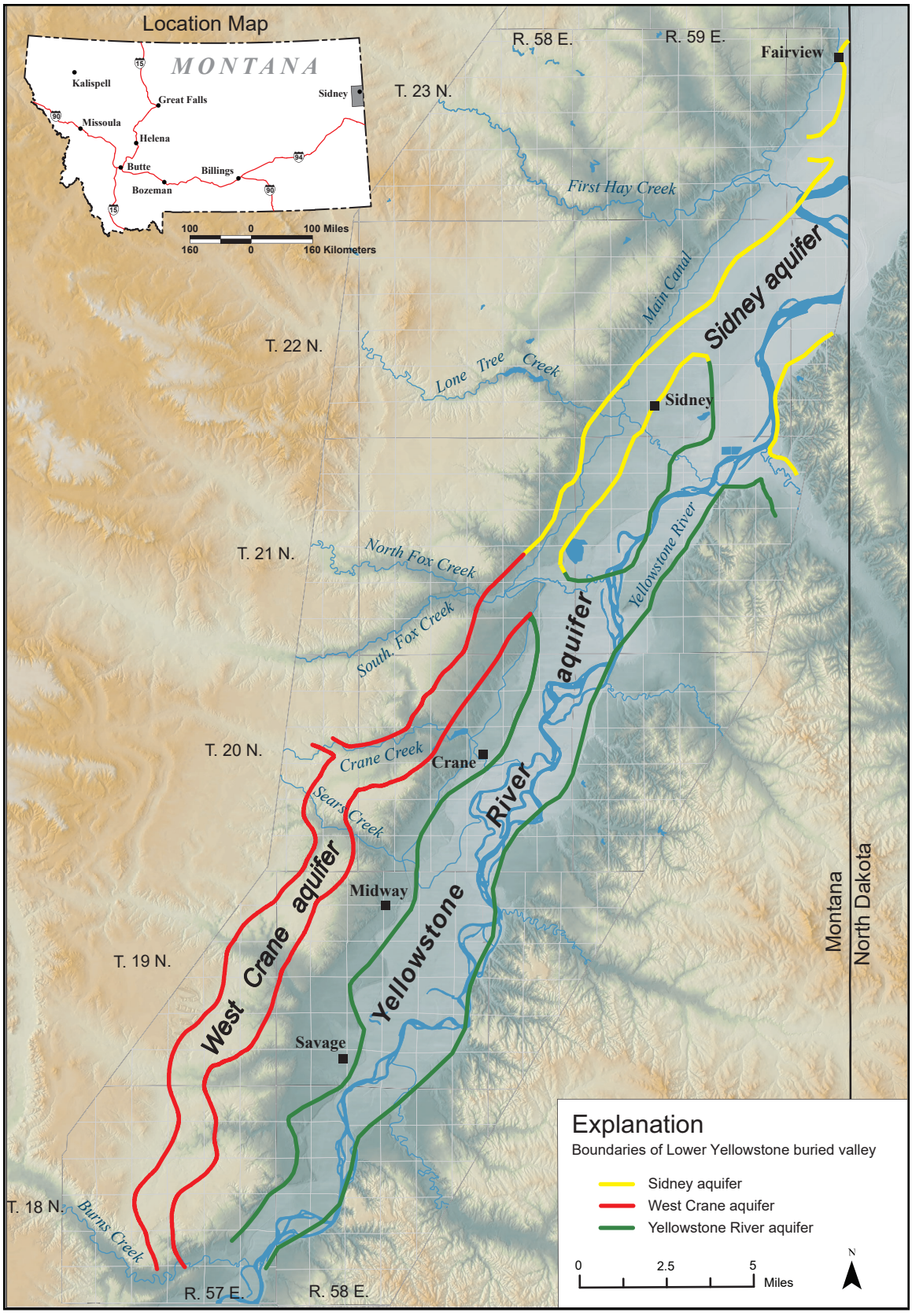

Figure 1. The Lower Yellowstone buried valley aquifer (LYBV) underlies the Yellowstone River valley and western valley slopes. The LYBV comprises three distinct segments: the Sidney aquifer and Yellowstone River aquifer, both of which underlie the valley, and the West Crane aquifer, which underlies the upland areas west of the Yellowstone River.

tion water and leakage from irrigation canals. Another part (the Yellowstone River aquifer), underlies the valley east of Sidney extending south to the county line. The southwestern part of the LYBV aquifer, the West Crane aquifer, extends from Fox Creek to Burns Creek, and underlies land higher in elevation (referred to as upland areas in this report) than the land irrigated using water from the Yellowstone River.

The West Crane aquifer is about 1 mi wide, occupying the basal sediments of a buried valley. The buried valley is up to 300 ft deep, and has a gradient similar to the modern Yellowstone River. The aquifer parallels and has a similar overall meandering pattern as the modern Yellowstone River valley; however, the land surface overlying the aquifer has little or no topographic expression of the buried valley. The primary study area is defined by the buried valley, but runoff from drainage basins to the west of the buried valley are important sources of recharge to the aquifer (fig. 2). The land surface west of the aquifer gradually slopes upward to drainage divides that mark the extent of the drainage basins potentially influencing the aquifer.

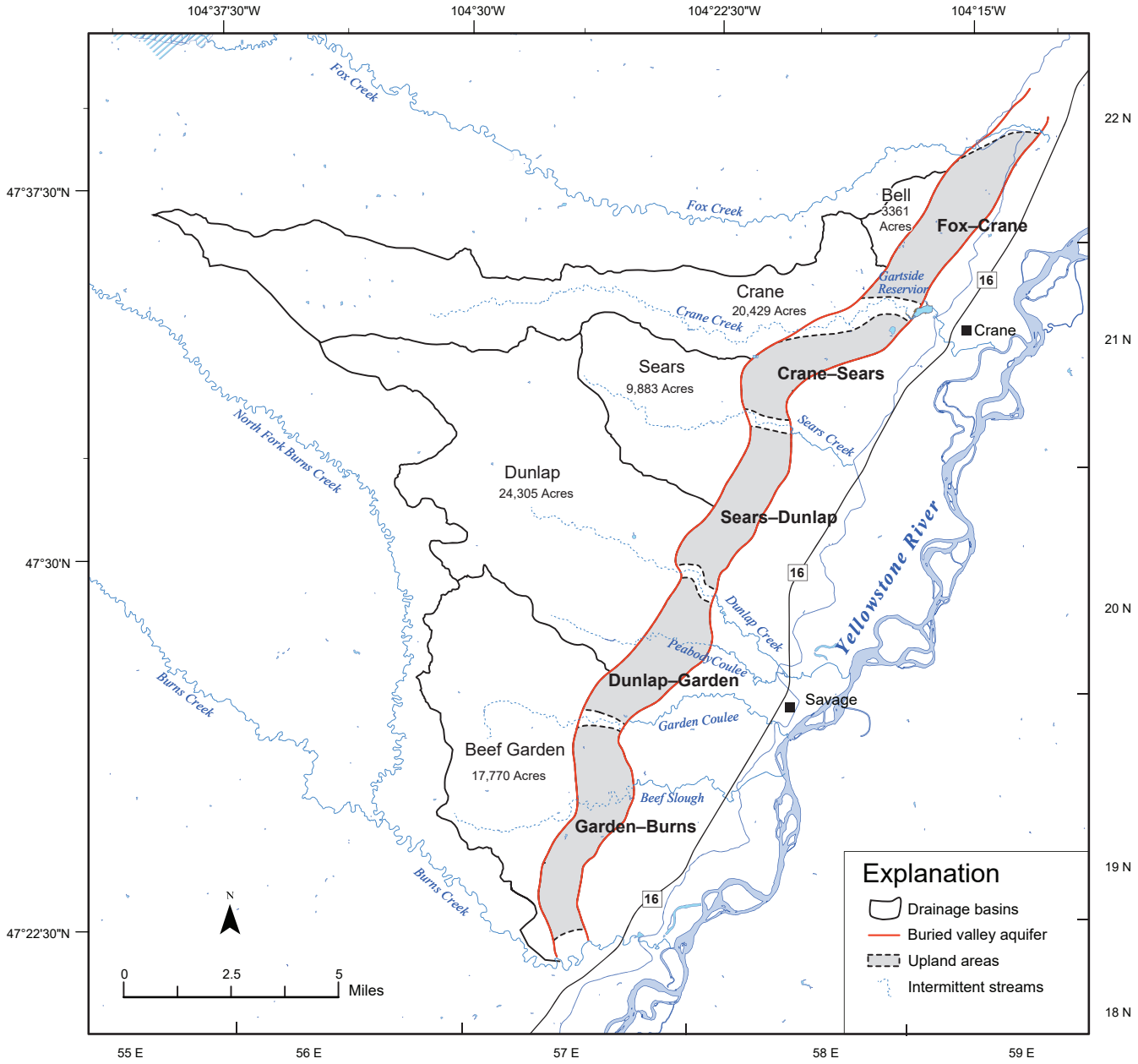

Figure 2. Project location showing the extent of the West Crane aquifer. Topographically higher drainage basins are to the west, and upland or interfluve areas overlie the aquifer (shaded). The upland areas are named from south to north based on the names of bounding stream valleys: Garden–Burns, Dunlap–Garden, Sears–Dunlap, Crane–Sears, and Fox–Crane.

Previous Investigations

The Sidney aquifer was discovered as part of the expansion of Sidney's water supply in the late 1960s and 1970s. This aquifer was informally named the LYBV during the source water assessment project by Miller and others (1998). Smith (1998) mapped a narrow band of thick unconsolidated deposits underlying the Yellowstone River valley from the North Dakota border southwest to Fox Creek.

Test drilling by the MBMG in the West Crane area funded by a Montana Department of Natural Resources (DNRC) irrigation development grant during the winter of 2006–2007 revealed that the LYBV extended under the uplands south of Fox Creek to Crane Creek. Prior to this the upland area was assumed to be underlain by Fort Union bedrock with no indication of a buried valley.

Test drilling by the MBMG in the fall of 2007, as part of a DNRC Renewable Resource Grant project, expanded the known aquifer extent from Fox Creek north to the North Dakota boundary near Fairview. A few test holes south of Fox Creek confirmed previous interpretations that the aquifer extended as far south as Crane Creek.

In 2009, irrigation wells were successfully completed in the West Crane area, verifying the existence of a productive alluvial aquifer. During the next few years, DNRC permitted three irrigation wells. Additional test drilling by the MBMG in 2013 expanded the known southern boundary of the aquifer southward to locations west of Savage (Reiten and Chandler, 2013, 2014, 2019). An initial groundwater model was developed in 2010 to assess the possible impacts of the first high-yield well on Crane Creek (MBMG, unpublished administrative report).

Physiography

The West Crane aquifer recharge area forms a triangular-shaped region that includes the watersheds of Beef Slough, Garden Coulee, Peabody Coulee, Dunlop Creek, Sears Creek, and Crane Creek, which are all tributaries to the Yellowstone River (fig. 2; Reiten and Chandler, 2023). The elevation of these watersheds gradually increases west of the aquifer, terminating at the divide located east of the North Fork of Burns Creek. The altitude at the divide is greater than 2,700 ft above mean sea level (amsl) at the highest position in the upper reaches of the Crane Creek watershed. The surface elevation overlying the aquifer ranges from about 1,930 ft to 2,240 ft amsl. At higher elevations west of the buried valley, the streams are intermittent (dry during some seasons when the water table drops below the elevation of the streambed) to ephemeral (dry except for periods of response to precipitation events, such as a rainstorm or snowmelt). Where they flow over the buried valley, the streams are ephemeral and typically form braided dry channels. Downstream and east of the buried valley, most of the streams are perennial or form permanent wetlands.

The upland areas between the tributaries (fig. 2) form broad low-relief landscapes, commonly mantled with soils developed in glacial till. These areas are favorable for irrigation development, compared to tributary drainages that have higher relief slopes and coarser grained soils. These uplands are named by the drainages they separate, from south to north, as Garden–Burns upland, Dunlap–Garden upland, Sears–Dunlap upland, Crane–Sears upland, and Fox–Crane upland (fig. 2).

The West Crane aquifer has a basal elevation about 2,010 ft amsl at the southern end of the aquifer and is exposed above the level of Burns Creek (fig. 3; Reiten and Chandler, 2023). At the northern end of the aquifer, the basal elevation is about 80 to 100 ft below the land surface at Fox Creek (1,830 to 1,850 ft amsl). The uplands between tributary valleys range from about 100 ft to more than 200 ft higher in elevation then the tributaries that cross the aquifer.

Geology

The Paleocene Fort Union Formation crops out along valley margins at some locations and commonly forms rugged badlands topography. This formation is composed of poorly consolidated interbedded layers of sandstone, mudstone, siltstone, and lignite. The upper Tongue River Member of the Fort Union Formation underlies most of the West Crane study area. Near Burns Creek to the south, the lower Ludlow Member is at the surface, and is characterized by thinner bedded, finer-grained sediments containing smectite (swelling clays) that produce a characteristic "popcorn" weathering. The Fort Union Formation forms the bedrock base, overlain by Tertiary and Quaternary coarse-grained stream deposits and glacial till (Pritchard and Landis, 1975).

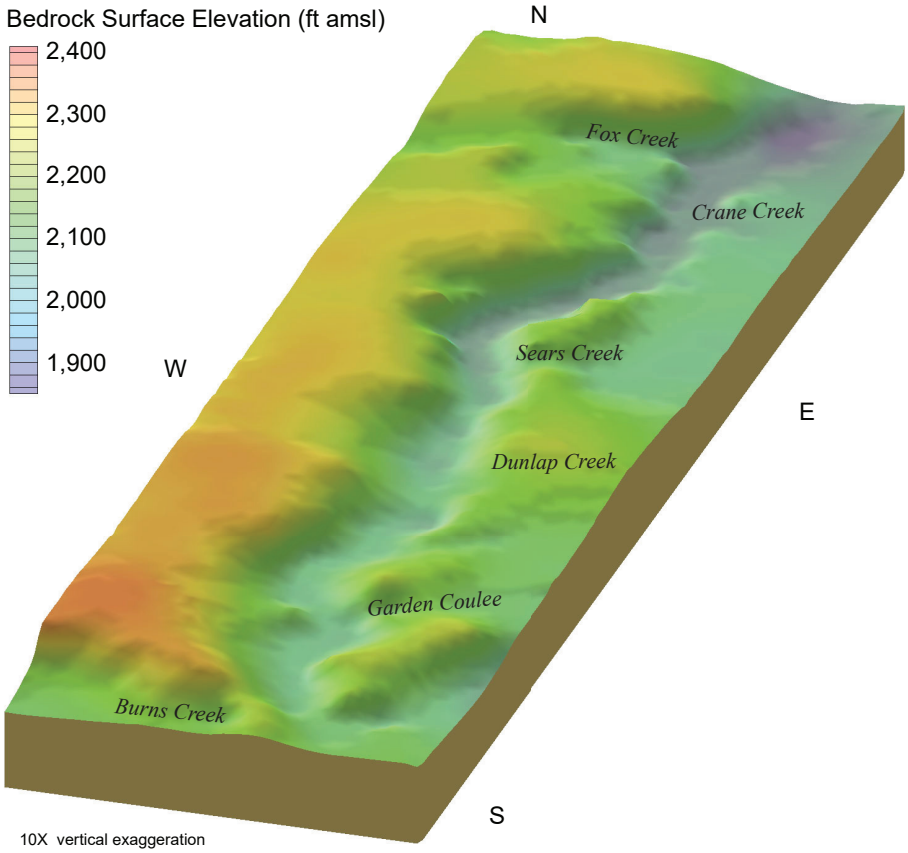

Figure 3. The buried valley bedrock surface containing the West Crane aquifer is shown in this schematic 3D image.

The Yellowstone River is flanked by stream terraces consisting of sand and gravel. The highest terraces are 760 ft above the modern river level west of Savage. This terrace is the oldest, with progressively younger terraces stepping down in elevation eastward. The age of these terraces ranges from Tertiary to Quaternary. The buried valley appears to be the ancestral Yellowstone River channel prior to the diversions of the Missouri and Yellowstone Rivers by Pleistocene glaciation. The modern Yellowstone valley formed following the retreat of the glaciers.

Climate

Richland County has a semiarid continental climate, characterized by cold, dry winters; cool, moist springs; moderately hot, dry summers; and cool, dry autumns. January is generally the coldest month, with an average low temperature of 2.1°F, and July the warmest month, with an average high temperature of 87.1°F (WRCC, 2021, based on 1905–2012 data). At Savage, the average precipitation is 13.86 in/yr based on 1906–2020 data (Reiten and Chandler, 2023). In most years, the majority of the precipitation falls during the growing season from May through August (fig. 4; Reiten and Chandler, 2023; WRCC, 2021, Savage, Montana Station 247382). Daily precipitation in 2019 (figs. 4, 5) was variable, with exceptional rain events occurring in September 2019. Annual precipitation is variable; between 2018 and 2020, the long-term normal was exceeded by 36% and 72% in 2018 and 2019 respectively. However, 2020 precipitation was 25% below the long-term normal.

DATA COLLECTION METHODS

Existing West Crane aquifer data, including driller-reported lithology and well yields, groundwater levels, water chemistry analyses, and aquifer test reports stored in the Ground Water Information Center (GWIC; https://mbmggwic.mtech.edu) database, were compiled and verified. Coal exploration borehole reports were also used to obtain lithologic information (available electronically at http://data.mbmg.mtech.edu/3D/DataViewer.asp?Database=4&focus=Menu&).

Data Management

Data generated during the project, including logs associated with exploration drilling and installation of monitoring wells, water-level measurements, water-quality data, aquifer test results, and streamflow mea-

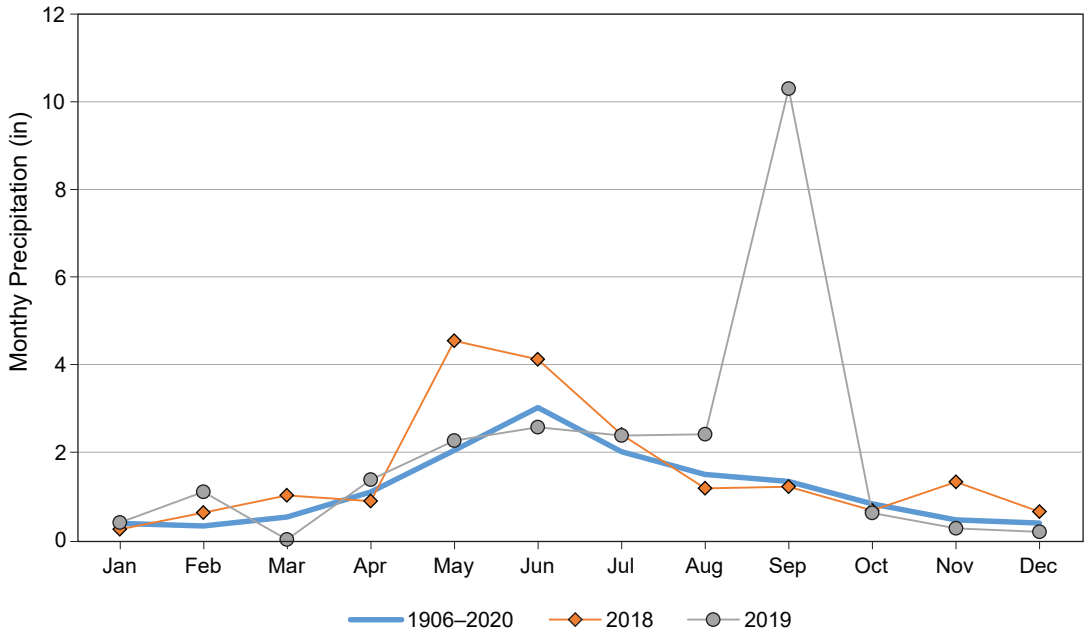

Figure 4. Comparison of monthly precipitation at Savage (WRCC, 2021). Note the exceptional rain events in September 2019 compared to average precipitation (1906–2020).

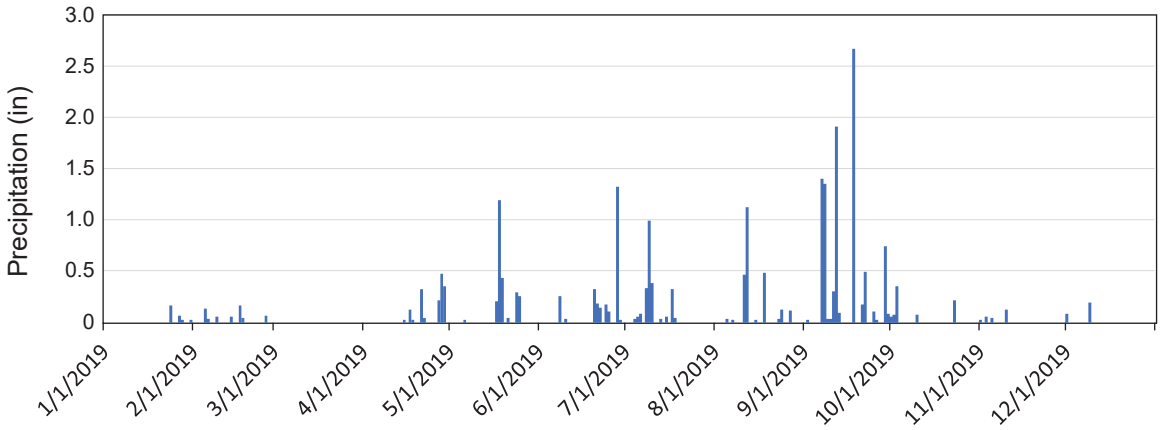

Figure 5. Daily precipitation at Savage, Montana (WRCC, 2021).

surements, are available from the GWIC database. All data are referenced to the GWIC identification numbers for wells (e.g., well 273787) and surface-water sites (e.g., site 305918).

Monitoring Network

We surveyed the elevations and coordinates of all monitoring and irrigation wells with a Leica 1200 GNSS Global Positioning System (GPS) system. The well survey utilized a base station and rover to provide 1-in accuracy for altitude and latitude–longitude at each location. Surface-water sites were located using a handheld GPS and elevations were determined from Google Earth.

Groundwater

A network of monitoring, stock, and irrigation wells provided seasonal and long-term water-level data for this project (plate 1 and appendix A included in Reiten and Chandler, 2023). Figures 6 (south section of the West Crane aquifer) and 7 (north section of the West Crane aquifer) show the locations of the wells used to construct the 2018 potentiometric map (Chandler and Reiten, 2020). We drilled 61 boreholes to determine the extent of the aquifer; 39 were completed as wells and are included as part of the monitoring network. The monitoring network consisted of 107 wells, 71 of which were equipped with data loggers. The water-level measurement frequency was variable; however, most data loggers were set to record hourly. Data loggers in monitoring wells adjacent to irrigation

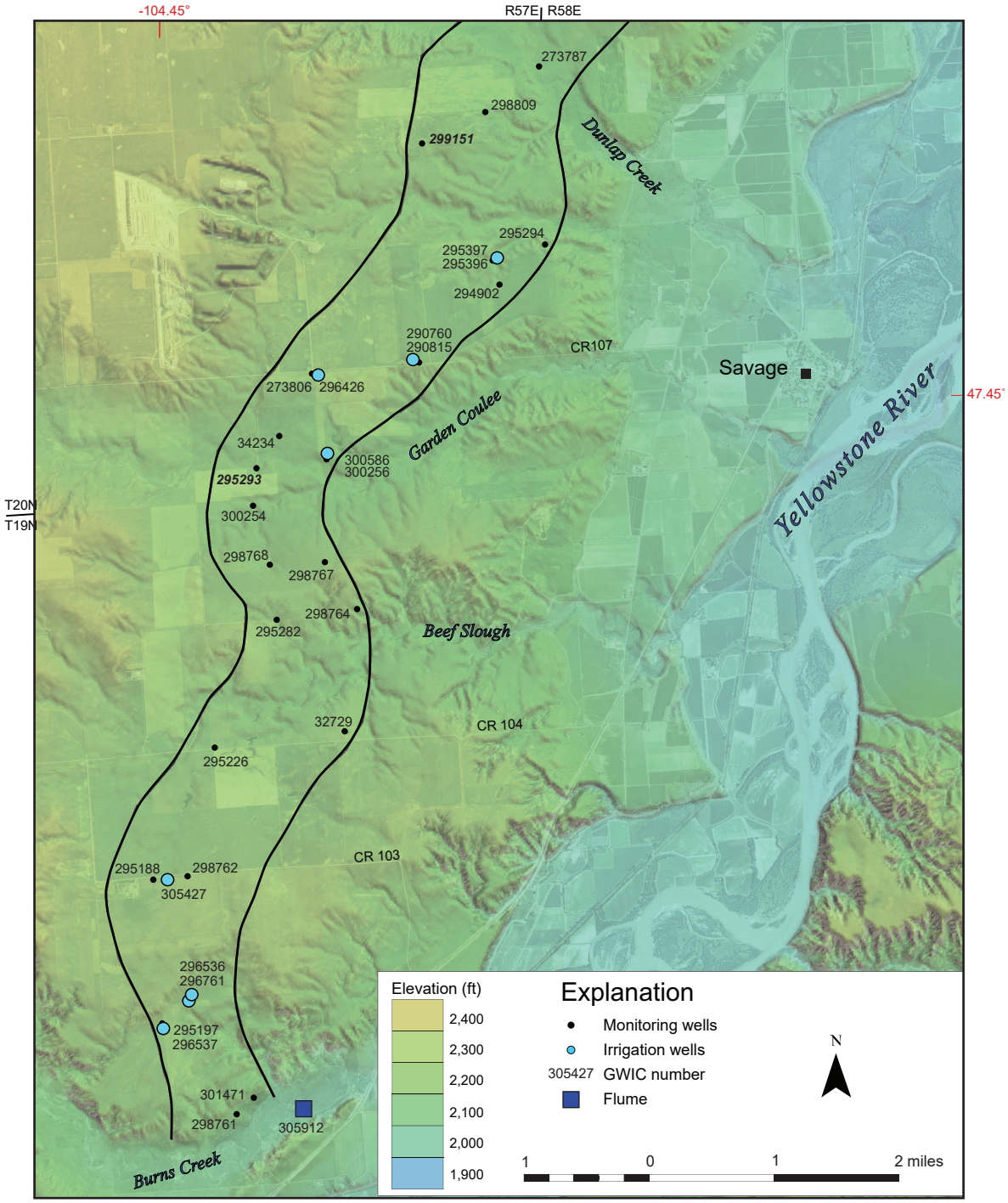

Figure 6. South section of the West Crane aquifer showing the distribution of selected monitoring wells, irrigation wells, and a surface-water flume. Wells for which calibration graphs are shown in figure 19 are in bold italics.

wells were set to record at 15-min intervals. Water levels in irrigation wells and stock wells were measured periodically, typically with a steel tape or sounder with an accuracy of 0.01 ft.

Irrigation water-use records for most wells were obtained from irrigators who control their systems remotely using the AGSENSE system (www.wagnet.net). In addition to turning pivot systems on and off, AGSENSE stores daily water use data.

Surface Water

To assess potential groundwater contributions to streamflow, we installed cutthroat flumes on Burns Creek (site 305912, fig. 6), Crane Creek, and Sears Creek (sites 305918 and 305915, respectively, fig. 7), near where these creeks cross the eastern boundary of the West Crane aquifer. Dunlap Creek forms a channel similar in size and gradient to Sears Creek, but access to the site was unavailable. The flume on Crane Creek

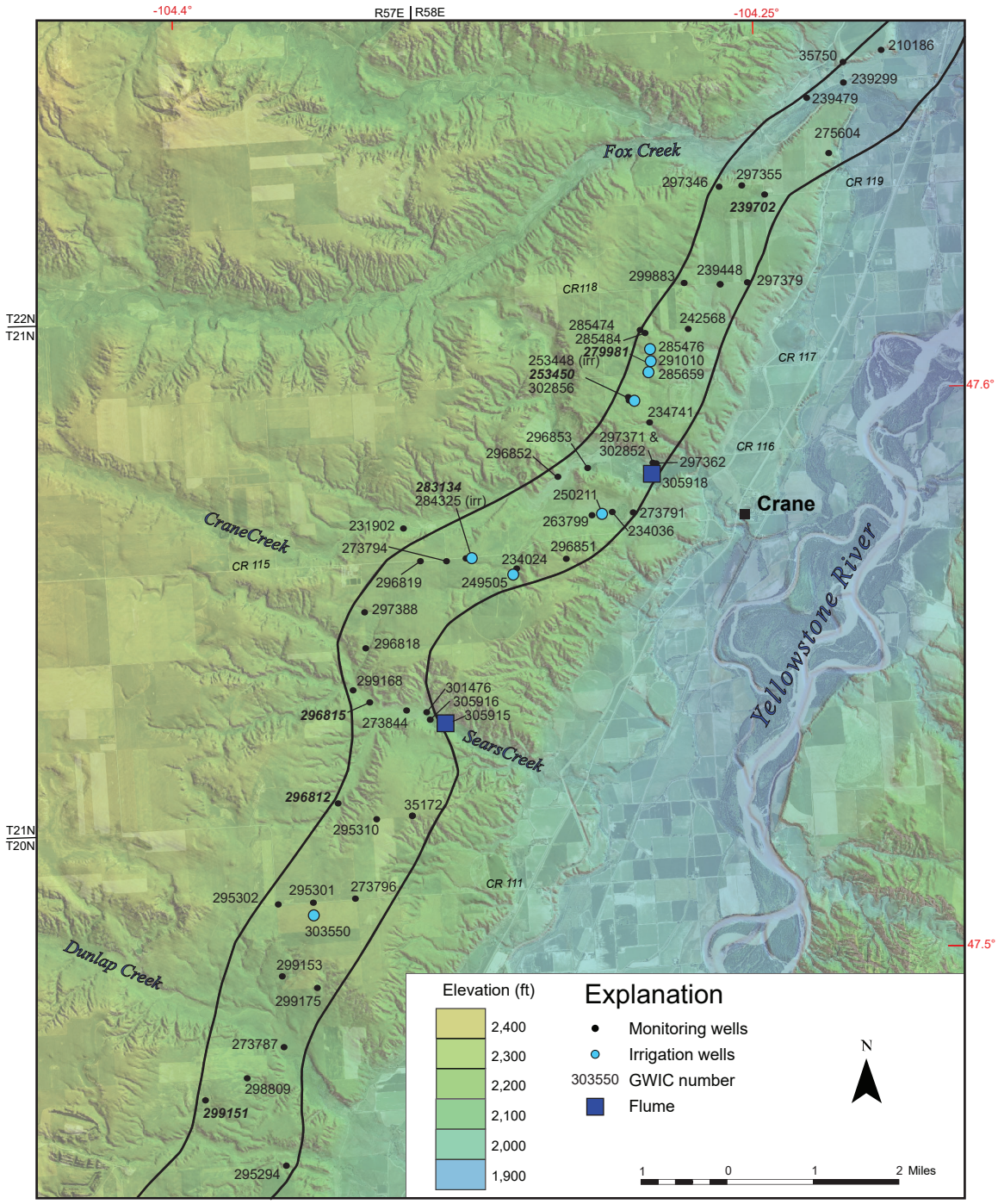

Figure 7. North section of the West Crane aquifer showing the distribution of selected monitoring wells, irrigation wells, and two surface-water flumes. Wells for which calibration graphs are shown in figure 19 are in bold italics.

measures flow out of a drainage system installed by Montana Fish, Wildlife and Parks in the 1980s. The flume on Sears Creek measures flow near the downstream edge of the buried valley where surface flow starts. The Burns Creek flume measures flow downgradient from where the Creek crosses the aquifer. Data loggers in the flume stilling wells recorded stages hourly.

Aquifer Test Data

To determine the West Crane aquifer hydraulic characteristics, aquifer test data from 14 water-permit applications were analyzed using AQTESOLV (Duffield, 2007) and summarized in Reiten and Chandler (2021).

Hydrogeologic Framework

The geologic and hydrogeologic framework presented in Reiten and Chandler (2023) were used in

developing stratigraphic cross sections, aquifer maps, and a hydrogeologic conceptual model.

In addition, shallow piezometers were installed in six hand-augered boreholes. All information about the monitoring wells, boreholes, and piezometers, including location and lithologic logs, are available from the GWIC database at https://mbmggwic.mtech.edu and in appendix A of the hydrogeologic report (Reiten and Chandler, 2023).

CONCEPTUAL MODEL

The West Crane aquifer occupies an ancestral river valley that was incised into fine-grained Fort Union Formation (fig. 3). The Fort Union Formation bedrock, with its low permeability, limits the lateral flow and defines the shape of the buried valley aquifer.

The bedrock valley walls act to trap groundwater in the unconsolidated valley-fill materials, conceptually creating a "fill and spill" aquifer (fig. 8; Reiten and Chandler, 2023). The aquifer is a sand and gravel deposit at the base of the buried valley that ranges in thickness from less than 15 to about 50 to 60 ft. Overlying the aquifer are till and outwash materials that include layers of silty sand and clay, interbedded with minor sand and gravel layers. These overlying materials cause the basal aquifer to be in a confined to leaky confined condition (fig. 9).

Groundwater and Surface-Water Flow Systems

The aquifer is recharged (fill) by infiltration of precipitation, streamflow loss from the tributary creeks, and lateral groundwater inflow. Groundwater discharges (spills) through notches eroded into the east side of the aquifer where the creeks cross the bedrock valley, and at the north and south ends of the valley. At the southern end, the aquifer gravels are cemented, acting as a plug that keeps heads about 60 ft higher in the aquifer than in Burns Creek. At the northern end, groundwater discharges to a large wetland area and to the Sidney aquifer. At all the discharge sites, where groundwater levels are close to the surface, water is lost to evapotranspiration (ET).

Sears Creek and Dunlap Creek are intermittent streams on the west, upgradient side of the buried valley, but form perennial streams near the east, downgradient boundary. Other tributary streams develop wetlands near the eastern edge of the buried valley where

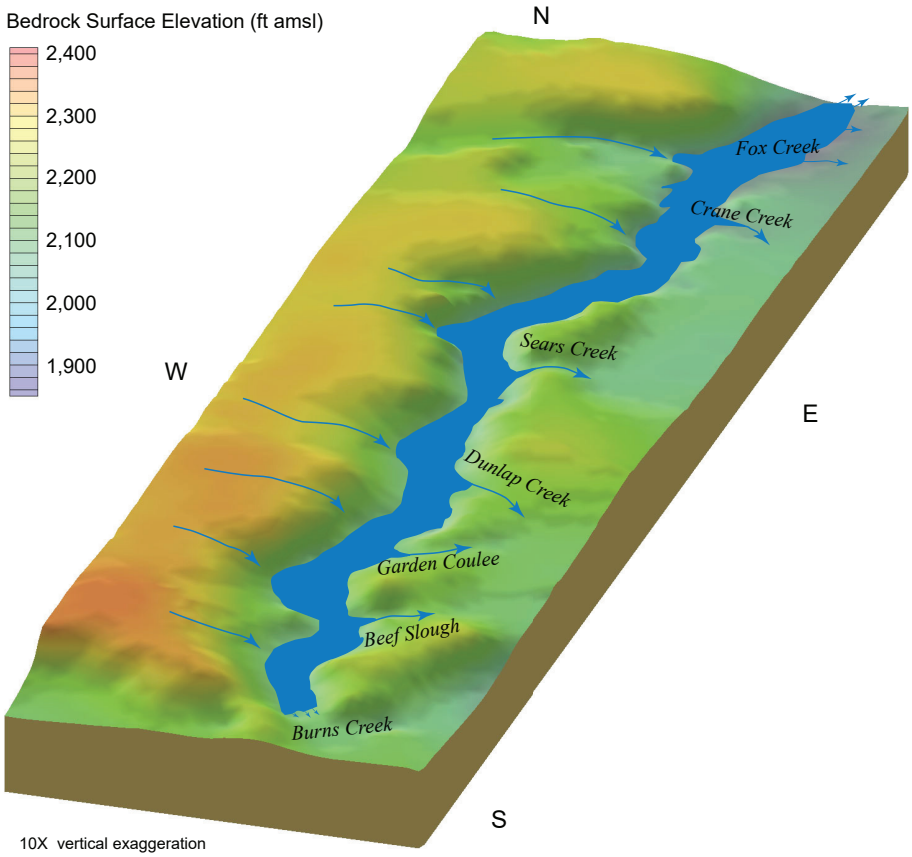

Figure 8. Schematic showing the fill and spill conceptual model. "Fill" is groundwater recharge into the aquifer and "Spill" is groundwater discharge from the aquifer.

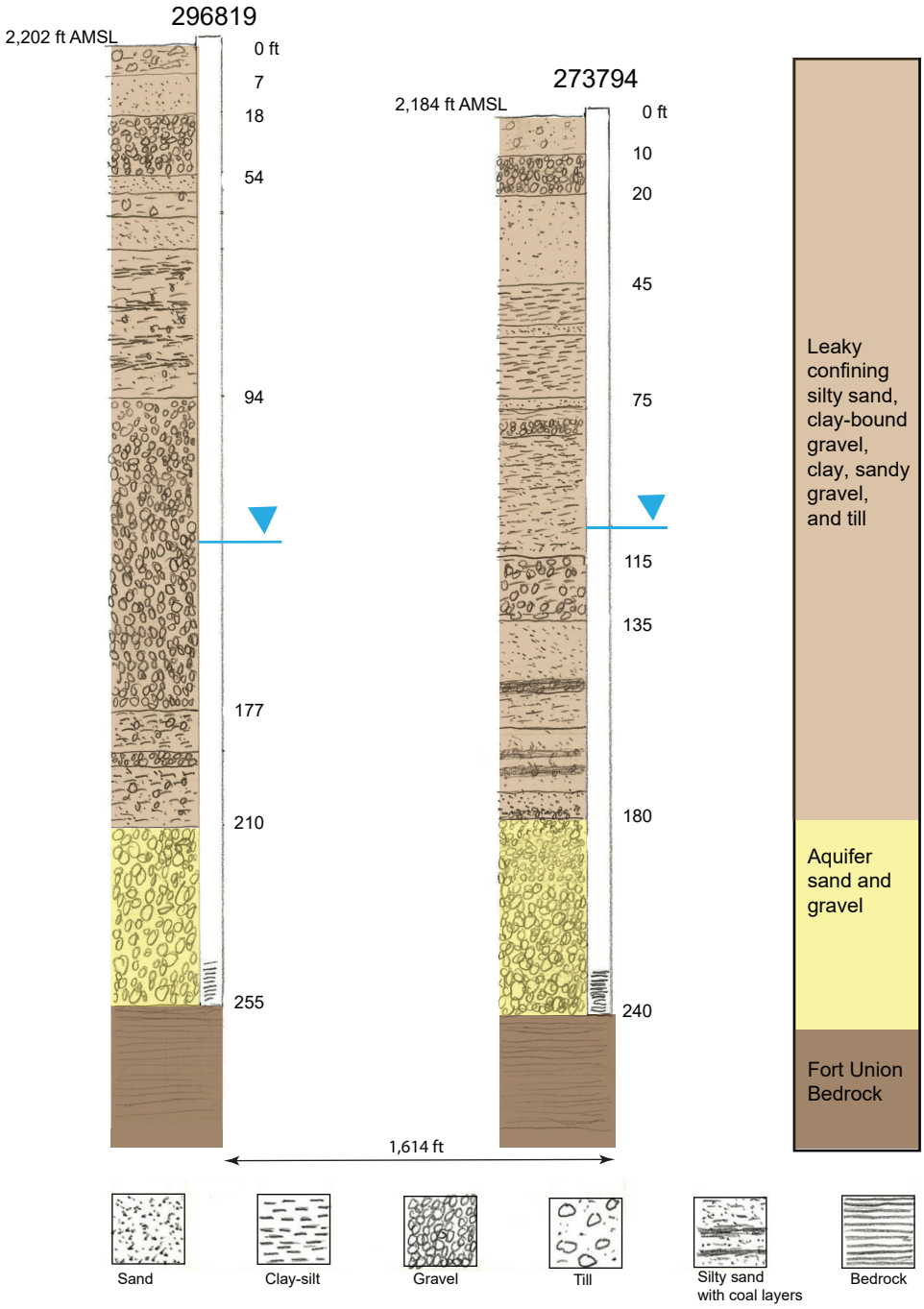

Figure 9. Well logs from two monitoring wells installed south of Crane Creek show the typical semi-confining layer heterogeneity recorded in the West Crane aquifer (modified from Reiten and Chandler, 2023).

groundwater spills out of the aquifer. The flow to the tributary streams depends primarily on the elevation of the notch eroded into bedrock along the east edge of the buried valley. Flows in Sears and Dunlap Creek are similar at about 0.5 to 1 cfs due to the similarity of the potentiometric surface in relation to the elevation of the bedrock notch.

Potentiometric Surface

A groundwater divide about 4.5 mi north of Burns Creek separates flow to the north towards Fox Creek and flow to the south towards Burns Creek (fig. 10). South of the groundwater divide the hydraulic gradient is low, as indicated by the small change in water levels over long distances. The gradient increases near Burns Creek, with a 60 ft drop between the last contour and the creek 600 ft away. In this area the cemented sands and gravels form a barrier to groundwater flow. Groundwater discharges to wetlands, seeps, and springs.

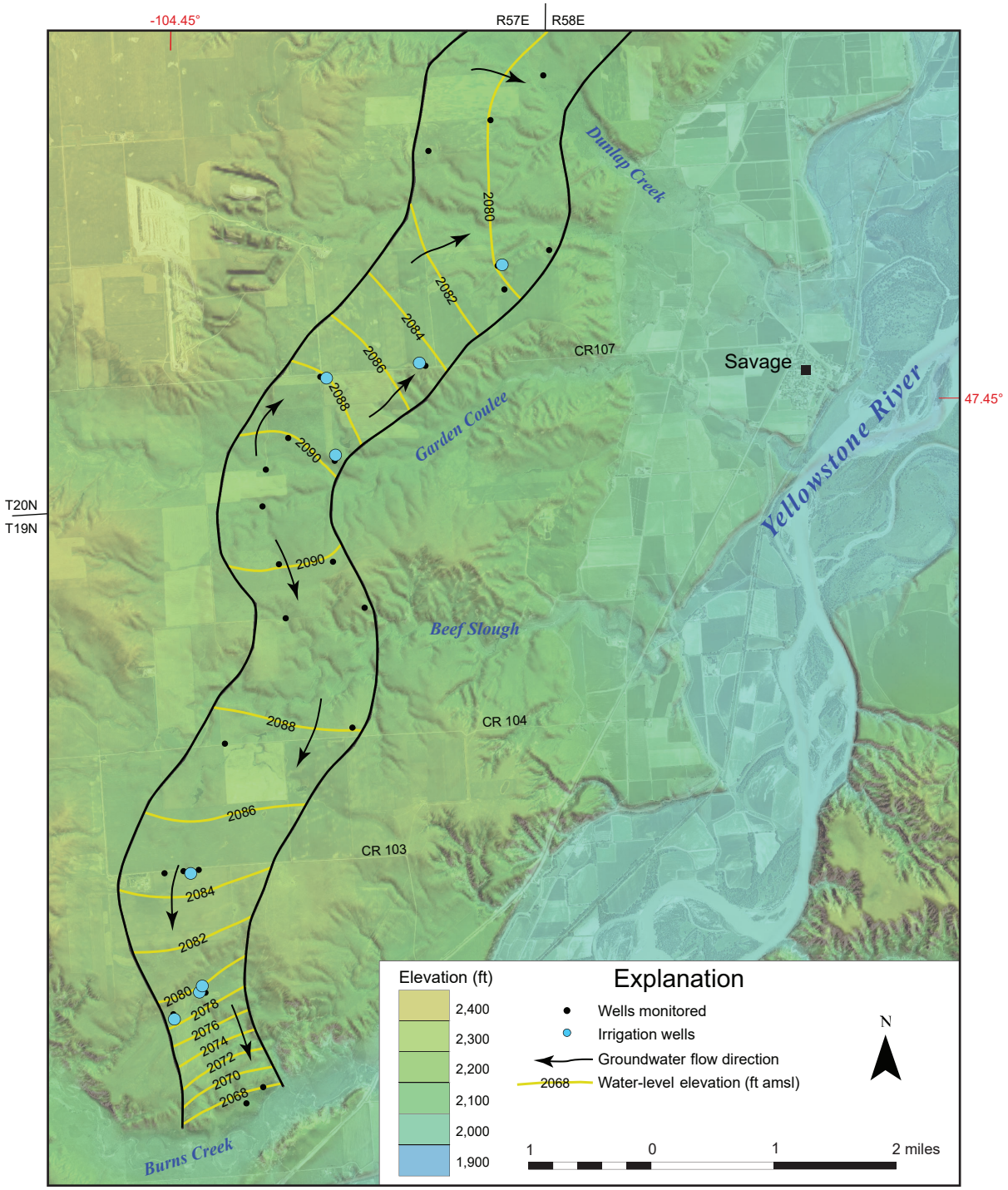

Figure 10. South section of the West Crane aquifer showing the potentiometric surface contours and groundwater flow directions. Notice the groundwater divide near the center of the figure.

Groundwater in the northern section of the West Crane aquifer flows northward, with alternating gradients (fig. 11). Steep gradients typically indicate areas where the aquifer has lower transmissivity (ability to transmit water), compared to locations where the gradient is relatively low, and the aquifer has greater transmissivity.

Groundwater also flows to the east towards the Yellowstone River through shallow alluvial aquifers underlying the tributaries.

Aquifer Properties

Aquifer test results from 14 wells completed in the basal sand and gravel provide a range of transmissivities from about 4,000 to 35,000 ft^2/d and storage coefficients ranging from 0.0001 to 0.03. Some of the

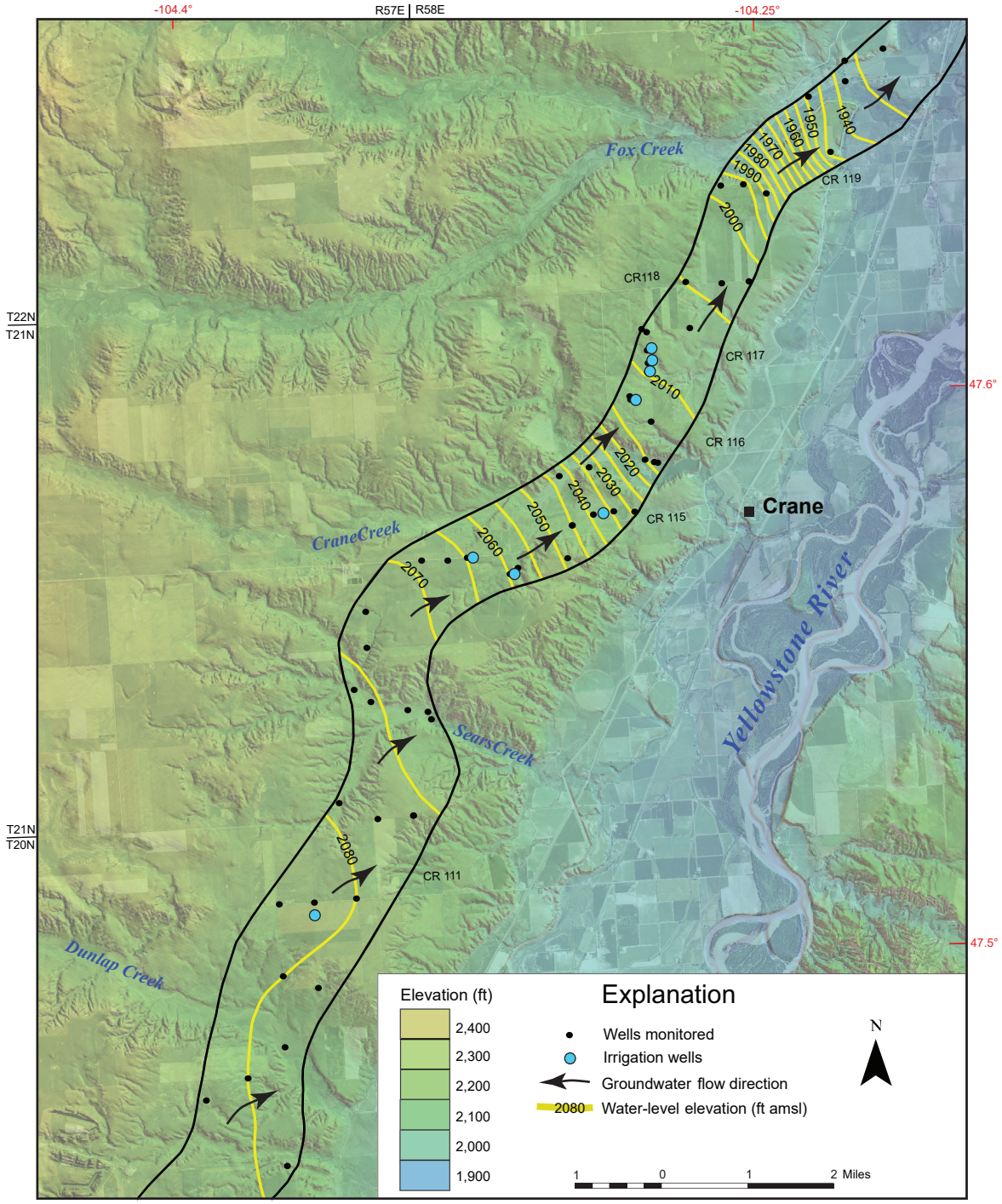

Figure 11. North section of the West Crane aquifer showing the potentiometric surface contours and groundwater flow directions.

tests were conducted near aquifer boundaries, so those results are somewhat less certain, though boundary conditions were applied in the analyses of these tests. Overall, the median value of transmissivity is about 23,760 ft^2/d (Reiten and Chandler, 2023). Estimated hydraulic conductivity values ranged from 360 ft/d to 1,100 ft/d, with a median value of 910 ft/d and a geometric mean of 800 ft/d. The details of aquifer testing are presented in the aquifer test summary report (Reiten and Chandler, 2021) and discussed further in Reiten and Chandler (2023).

Groundwater Budget

The groundwater inflows (recharge) and outflows (discharge) for the West Crane aquifer were estimated based on field data collected during 2019 and precipitation data from 2011 through 2020 (fig. 12). The derivation of the inflow and outflow components is

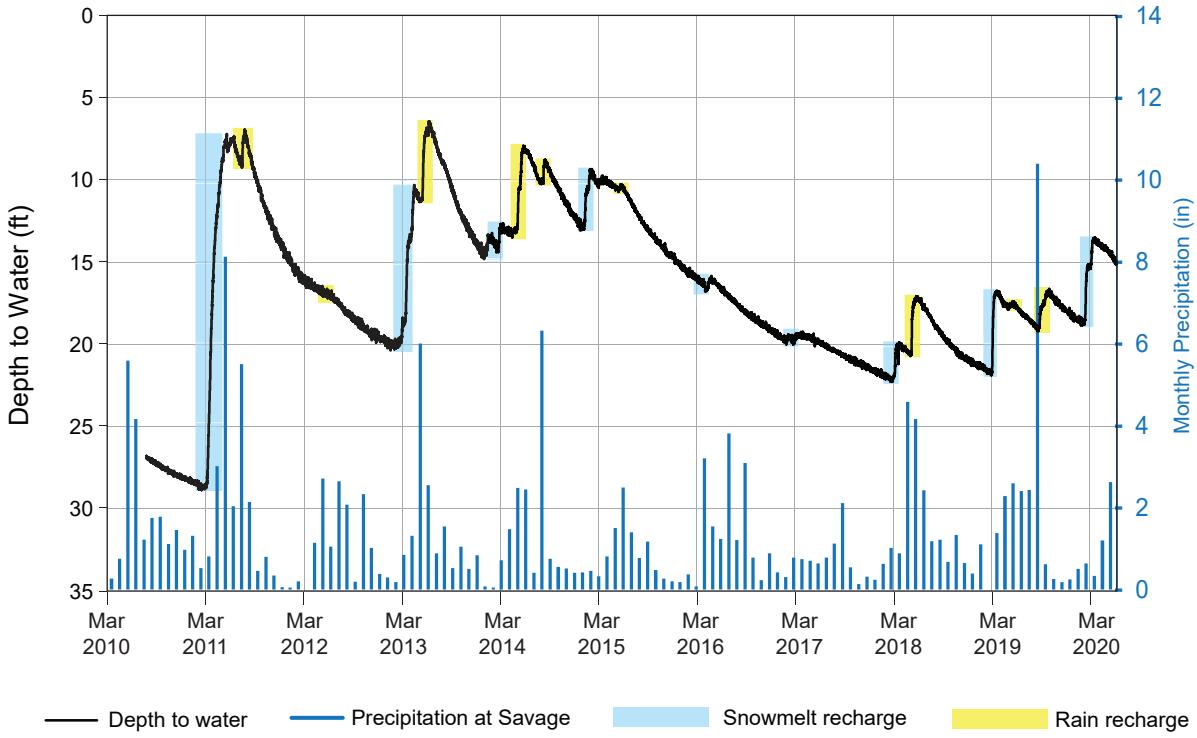

Figure 12. Water levels in well 231902 show greater recharge from snowmelt than rain events for the 10-yr period 2010–2020 (WRCC, 2021).

included in Reiten and Chandler (2023) and summarized in table 1. The groundwater flow into and out of the West Crane aquifer was estimated for a range of possible recharge and discharge amounts. The groundwater budget for the aquifer is:

$$R + GW_{in} = ET + PW + GW_{out},$$

where:

Inflows

R is recharge (% of precipitation), and GW_{in} is groundwater inflow at aquifer margins.

Outflows

ET is evapotranspiration, PW is pumping wells, and GW_{out} is groundwater outflow at aquifer margins.

The range of inflows and outflows presented in this section helped guide model development. The final groundwater budget is a derivation of field data and model results.

Inflows

The aquifer is recharged through infiltration of rainfall and snowmelt, and groundwater flows into the aquifer system from the upgradient margins of the aquifer. The stream channels crossing the aquifer are usually dry, and only flow during large runoff events from rapid snowmelt or exceptional rainfall. The exposed sand and gravel in these channels allow for the rapid infiltration of runoff into the aquifer. The watersheds drained by these tributary streams cover an area many times greater than the land overlying the aquifer. Darcy flow methods were used to estimate groundwater flow into the aquifer at the upgradient aquifer margins and where the small streams cross the aquifer.

Measuring the periodic flows in the tributaries was impractical. Therefore, we relied on snowmelt and precipitation data combined with PEST to help refine the water budget. An episodic master recession technique (Nimmo and Perkins, 2018) was used to relate snowmelt and precipitation events to observed water-level responses and estimate the recharge to precipitation ratios for a given location. The results indicate that an estimated 5 percent of overall precipitation recharges the aquifer.

Well 231902 is completed in a buried tributary valley (located in the Crane Creek drainage) connected to the West Crane aquifer (fig. 7). The hydrograph for this well illustrates the groundwater response to precipitation and snowmelt recharge typical in upland areas (fig. 12). Water levels rise during the spring snowmelt following years of appreciable snowfall, notably in

Table 1. Annual groundwater budget for the West Crane aquifer based on field data and interpretations.

Inflow		
Budget Component	Low Estimate (acre-ft/yr)	High Estimate (acre-ft/yr)
Rainfall recharge	0	10,100
Snowmelt recharge	2,020	30,300
Total Inflow	2,020	40,400

Outflow		
Budget Component	Low Estimate (acre-ft/yr)	High Estimate (acre-ft/yr)
ET	390	2,300
Net groundwater flow out at aquifer margins[a]	1,690	2,830
Streams	1,110	1,960
Pumping[b]	1,165	4,764
Total Outflow	4,355	11,854
Calculated Change in Aquifer Storage	-2,335	28,546

[a]Groundwater flows in from and out of the aquifer margins presented as the net outflow.
[b]Low pumping estimate represents 2019 reported irrigation pumping volume and high estimate represents 2019 irrigation season appropriated volume.

2011 and 2013. The high conceptual budget estimate for snowmelt recharge of 30,300 acre-ft/yr is based on the 2011 groundwater-level response. Groundwater levels also rise due to rainfall events during the later spring through fall, indicating recharge due to these events. The high conceptual budget estimate for rainfall recharge of 10,100 acre-ft/yr is based on the groundwater-level responses to multiple rainfall events in 2014. The groundwater-level responses to the high-intensity rainfall events in September 2019 were not as great. These lesser responses indicate these events generated more overland runoff than groundwater recharge compared to other rainfall events. Note that the combination of high snowmelt and rainfall recharge events occurring in a single year may be uncommon. Drier winters are evident in the lack of spring recharge for 2012, 2016, and 2017, resulting in a much lower (2,020 acre-ft/yr) low conceptual budget estimate for snowmelt recharge. The lack of discernable groundwater-level responses to rainfall during 2016 and 2017 results in a low conceptual budget estimate of zero rainfall recharge. The slow water-level decline following recharge events suggests a delayed movement of water from the surface through the leaky aquifer materials overlying the buried valley aquifer. Reiten and Chandler (2023) provide a detailed description of groundwater response throughout the aquifer.

Outflows

Groundwater discharges from the aquifer as stream baseflow, outflow at the aquifer margins, well withdrawals, and through evapotranspiration (ET) in riparian areas. Estimates of outflows are presented in the hydrogeologic report (Reiten and Chandler, 2023). Tables in that report provide detail on ET ranges and groundwater flow out of the aquifer. Again, Darcy flow methods were used to estimate groundwater flow out of the aquifer at downgradient margins and where the small streams cross the aquifer.

Irrigation water use is compiled in the interpretive report, and includes general information on the timing and increase in irrigation withdrawals since the first well was put into use in 2011 (Reiten and Chandler, 2023). As of March 2021, permitted irrigation appropriations totaled 5,041 acre-ft annually. However, ac-

tual use is much less. In 2019, the total irrigation withdrawals were about 1,165 acre-ft, compared to 3,691 acre-ft appropriated at that time (Reiten and Chandler, 2023). The 2019 data are referenced because that is the year the 1-yr transient model version is based on. The actual versus appropriated water volumes for the years 2011 through 2020 are presented in Reiten and Chandler (2023; refer to table 10 and fig. 25).

In 2019, there were records of 10 domestic and 21 stock wells withdrawing an estimated 65 acre-ft/yr from the aquifer (Reiten and Chandler, 2023), representing about 5 percent of the total groundwater withdrawals.

Changes in Storage

Groundwater storage values span a wide range depending on conditions in a given time period, and are controlled by irrigation pumping and recharge events from snowmelt or rainfall. Our estimates calculated as the differences in the other inflow and outflow terms of the groundwater budget range from modest storage losses associated with drought and groundwater withdrawals to large gains in wetter years.

NUMERICAL MODEL CONSTRUCTION

The West Crane aquifer groundwater model included steady-state and transient versions developed using MODFLOW (see Software Descriptions section below); PEST was used to estimate input parameter values to calibrate the model to measured groundwater levels and estimated baseflow values (Doherty and Hunt, 2010). The steady-state model version was based on late winter/early spring conditions observed in March 2018. The transient model version included a 1-yr simulation based on 2019 information and used PEST to refine the hydraulic conductivity, storage, recharge and streambed conductance. The 1-yr transient model was used for modeling the water use scenarios. Finally, the construction of the steady-state and 1-yr transient versions were made consistent with each other, and a final calibration of the model hydraulic conductivity and storage parameter input values was performed using PEST. Modeling files are provided for the final steady-state and 1-yr transient versions of the model, and are available for download from the MBMG website for this publication, https://doi.org/10.59691/OZVN9020.

Software Descriptions

We initially used the U.S. Geological Survey (USGS) MODFLOW-2000 code, version 1.19.01 (Harbaugh and others, 2000), with Groundwater Modeling System (GMS) version 7.0 (Aquaveo, 2009). GMS 10.4 (Aquaveo, 2019) using MODFLOW 2005 was used to adapt the steady-state model for initial transient simulations (Harbaugh, 2005). These initial model constructs were calibrated using PEST version 14.01 (Doherty, 2016). The steady-state and 1-yr transient model versions were upgraded to MODFLOW 6 using Groundwater Vistas version 8 (ESI, 2020), and final calibration of the hydraulic conductivity and storage input parameter values of both versions was jointly performed using PEST_HP 17.42 (Doherty, 2021).

Model Domain

The known extents of the buried valley aquifer form the basis for the model domain. The model surface was defined using ground-surface elevations. The model has two layers: (1) the upper model layer represents the semi-confining layers overlying the buried valley aquifer and is composed of glacial till, modern stream alluvium, and other surficial sediments; and (2) the lower model layer represents the West Crane aquifer and the Fort Union bedrock west and east of the aquifer. The West Crane aquifer is represented in the middle polygon in layer 2. The long, narrow polygons on each side of the aquifer representing bedrock are about 11 mi^2 each (fig. 13).

The bottom of layer 2 represents the top of the Fort Union Formation beneath the buried valley sediments. The bottom of layer 1 and top of layer 2 represent the top of the buried valley aquifer and the bottom of overlying glacial deposits including till and outwash. These surfaces were created in GMS using lithologic data from water well logs and information from the coal database.

Spatial Discretization

The two-layer MODFLOW grid was constructed with 630 rows and 115 columns of 200 by 200-ft cells rotated approximately 24° east of north. The exact rotation of the model grid and the X- and Y-coordinate values of the model grid origin are provided in the MODFLOW 6 Discretization Package input files for the models. A model boundary polygon was used to

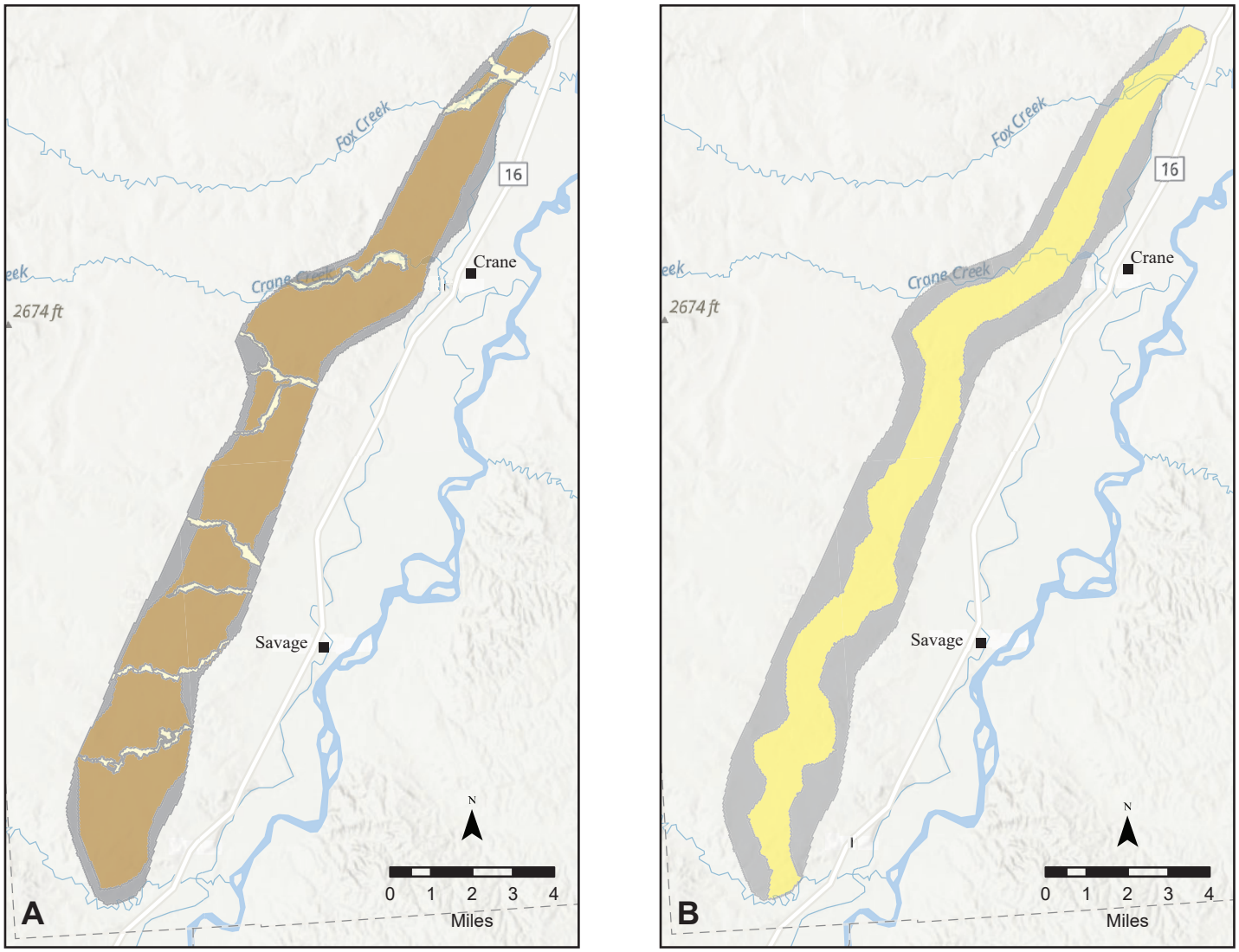

Figure 13. These images show polygons of hydrostratigraphic units used for developing spatial distributions of input values of hydraulic conductivity (K), specific storage (S_s), and specific yield (S_y) in layers one (A) and two (B) of the groundwater model. (Note that a pilot point was also used to create hydraulic conductivity value of 0.5 ft/d for the cemented zone at the southern end of the West Crane aquifer).

select the 63,854 active cells from the grid total of 144,900. The projection was set to Montana State Plane coordinates, North American Datum 1983, with units of International Feet. The vertical datum is NAVD88.

Temporal Discretization

Steady-State and Transient Model Versions

The steady-state model version represents a single unit-time stress period, which is simulated as a day. This setup is strictly a presentation of typical, long-term stream baseflow conditions per unit day and not any specific date. For steady-state simulations, we utilized average annual boundary conditions, calculated as daily rates. The steady-state model does not include transient conditions such as pumping from wells during the irrigation season nor changes in storage. The model was subsequently calibrated to March 2018 groundwater-head data. This steady-state version of the model may be used for certain applications, such as rapidly estimating how the system may respond overall to long-term changes in recharge, adding time-averaged pumping, or other changes in the groundwater budget.

The 1-yr transient model was based on 2019 field conditions, with an initial steady-state stress period followed by 365 daily transient stress periods. This 1-yr transient model version is the most useful tool to evaluate the effects from future irrigation wells.

Hydraulic Parameters

The layers 1 and 2 model polygons and the hydraulic conductivity ranges are shown in figure 13. In the steady-state model, layer 1, the largest polygon in the central area is denoted as glacial till and fine-grained deposits with hydraulic conductivity values between 0.0025 ft/d and 8 ft/d (fig. 13A). The thin, generally east–west-oriented polygons represent modern stream alluvium deposits as mapped on plate 2 of Reiten and Chandler (2023), with higher hydraulic conductivity values of 2 ft/d to 200 ft/d. The thin polygons around the margins are all denoted as Fort Union bedrock, with a hydraulic conductivity value of 0.1 ft/d.

In layer 2, the largest central polygon represents the West Crane aquifer, consisting of the deep sand and gravel buried valley aquifer (fig. 13B). This polygon shows the geometry of the main aquifer in the model, with areas extending approximately ½ mi on each side of the central polygon representing the surrounding Fort Union bedrock. Hydraulic conductivities of the central polygon were generated using PEST and ranged from about 40 to 2,000 ft/d. For comparison, aquifer testing in the West Crane aquifer produced a range of estimated hydraulic conductivity values ranging from 360 to 1,300 ft/day (Reiten and Chandler, 2021). The simulated ranges are reasonable values based on aquifer testing and the expected range of sand and gravel deposits from literature (Woessner and Poeter, 2020). The Fort Union bedrock polygons west and east of the West Crane aquifer were assigned hydraulic conductivity values of 0.1 ft/d. A PEST pilot point in layer 2, in the vicinity of the cemented sands and gravels north of Burns Creek, was assigned a hydraulic conductivity value of 0.5 ft/d.

The West Crane buried valley aquifer is generally fully saturated, so the primary component of aquifer storage is related to compressibility of the aquifer materials and water itself and is known as specific storage (S_s). Note that S_s has units of 1/length because it represents volume of water per unit of aquifer per unit of head. For a fully saturated aquifer, the overall storativity of the aquifer is calculated as the S_s multiplied by the aquifer thickness (b): (S_s x b). The analyses of West Crane aquifer tests produced estimates of total storativity ranging from 0.0001 to 0.03 (dimensionless; Reiten and Chandler, 2021). When the estimated storativity values for each test location are divided by the local aquifer thickness, the derived S_s values range from 4.5 x 10^{-6}/ft to 0.0011/ft. The modeled S_s input values estimated by PEST for the 2019 transient model version described below ranged from 1.6 x 10^{-5}/ft to 3.0 x 10^{-4}/ft. Note that these values fit within reported literature values for loose sand, dense sand, and dense sandy gravel that range from 1.5 x 10^{-4}/ft to 3.1 x 10^{-4}/ft (Batu, 1998). The Fort Union Formation bedrock in layer 2 of the model was also simulated to be generally fully saturated. Literature values for unfractured bedrock are generally less than 1 x 10^{-6}/ft (Batu, 1998). As such, the input value for S_s of the Fort Union Formation bedrock was set to 1 x 10^{-7}/ft.

The fine-grained and alluvial sediments modeled in layer 1 are not fully saturated and considered as unconfined units. While compressible storage still

occurs in these units, pore space that can be filled and then drained due to gravity is generally several orders of magnitude greater than the compressible storage, and as such this porosity is the primary component of groundwater storage. This drainable/fillable porosity is known as specific yield (S_y), which is dimensionless because it represents the volume of water drained per unit volume of the porous aquifer material. There are no measured S_y values in the model area, so literature-reported values were used to guide PEST to estimate model input values (Batu, 1998). For the till and other fine-grained deposits, the estimated S_y values ranged from 0.01 (1%) to 0.12 (12%). For the stream alluvium, the estimated S_y values ranged from 0.05 (5%) to 0.22 (22%). Input-S_y values for model cells representing Fort Union Formation bedrock were set to 0.015 (1.5%). Note that the model also requires input values for model cells representing the West Crane aquifer sand and gravel, though the S_y storage would only be relevant to the model results should the simulated water table fall below the top of the aquifer. S_y values for the West Crane aquifer were set to a relatively conservative 0.15 (15%) based on the literature (Heath, 1983). Similarly, the model requires input values for S_s for the till and fine-grained materials and the stream alluvium, which were set to 3 x 10^{-4}/ft and 5 x 10^{-5}/ft, respectively (Batu, 1998).

Internal Boundary Conditions

Recharge (Inflows)

For the steady-state model, we used an initial recharge estimate of approximately 5 percent of average precipitation. The 1906–2020 average precipitation at Savage is approximately 1.2 ft/yr (13.9 in/yr), which gives an average daily value of 0.0033 ft/d (5% of that equates to 0.00017 ft/d). PEST estimated the spatially averaged recharge across the active model domain to be 0.00035 ft/d. Thus, the steady-state model PEST simulations increased the initial recharge estimate by a factor slightly greater than 2, equivalent to approximately 10.6% of the long-term average annual precipitation at Savage. The steady-state model represents March 2018, which includes a snowmelt recharge event that explains the higher recharge rate as a percentage of long-term average precipitation (fig. 12).

For the 2019 transient model version, recharge rates were differentiated between the areas where the tributaries cross the aquifer (lowland polygons) and the upland areas in between the drainages (upland polygons; fig. 14). The upland recharge rates were interpreted from delayed recharge responses in observation wells. Thus, the largest recharge values are associated with the March 2019 snowmelt event (fig. 15). Following snowmelt, recharge tapers off slowly, likely due to the variable and sometimes fairly deep connection with the water table. However, some summer precipitation events caused water-level increases. The unusual September 2019 high-precipitation event added late season recharge, with its own delayed recharge element, again tapering off over time. Winter recharge tapered off toward zero (fig. 15).

The lowland polygons have assigned recharge patterns that reflect a combination of snowmelt runoff in the late March time frame followed by spikes for each major precipitation event. From November through early March there is little assigned recharge, coinciding with the cold winter months when most precipitation simply accumulates at the surface as snow and ice.

Discharge (Outflows)

Riparian Evapotranspiration. The maximum evapotranspiration rate in the model area is estimated to be as much as 3 ft/yr during the summer months (Reiten and Chandler, 2023). Assuming a maximum ET rate of 3 ft/yr applies only to one quarter of the year (the summer months), and dividing that value by 365 days for the steady-state model condition results in an annually averaged value of 0.0021 ft/d. This value is assigned to relatively small-area polygons located where wetlands exist near where intermittent streams discharge near the east edge of the model area (fig. 14B).

ET for the transient model is applied from late March to mid-October in the ET polygons (fig. 14B). Maximum ET rate values range from less than 0.001 ft/d to 0.0057 ft/d (fig. 16). The maximum rates occur in late August. Reiten and Chandler (2023) provide a more detailed description of ET rates.

Groundwater Discharge to Streams. Groundwater discharge to streams was modeled using the MODFLOW Drain Package (fig. 14B). In the steady-state model version, flows were calibrated to estimated target values ranging from 9,600 to 115,508 ft^3/d (0.11 to 1.34 cfs). These values are generally comparable to

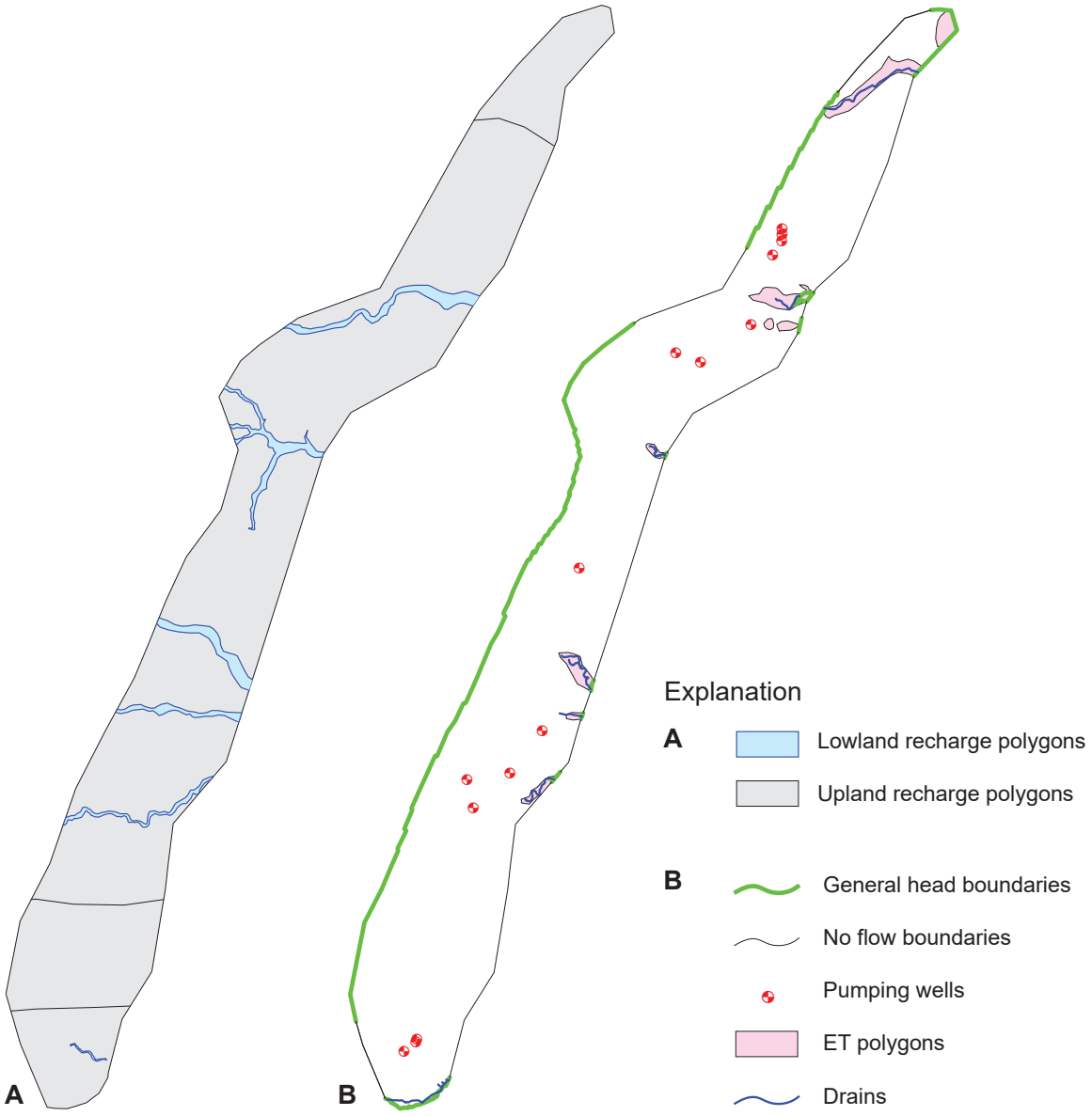

Figure 14. Model internal and external boundary features. Internal boundary features include the recharge polygons, pumping wells, ET polygons, and drains. External boundary features are no-flow boundaries and general head boundaries.

field data measured on Crane and Sears Creeks (Reiten and Chandler, 2023) that range from 0.22 to 1.14 cfs.

Wells. In the transient version of the model, the timing and pumping rates assigned to irrigation wells were based on the producer water-use records and nearby monitoring well data (Reiten and Chandler, 2023). The domestic and stock well withdrawals represent less than 5 percent of the total pumping (Reiten and Chandler, 2023), and therefore were not included in the model.

External Boundary Conditions

The potentiometric surface map (March 2018, Chandler and Reiten, 2020) was used to assign general head boundaries to cells around the edges of model domain at the aquifer margins (fig. 14B). The head values were assigned based on an interpolation of the potentiometric surface contours. These boundaries simulate groundwater flow in and out of the model domain.

Calibration

The steady-state model was initially calibrated using observed heads in monitoring wells and estimated discharges at springs and seeps; PEST was used to refine estimates for recharge, Drain Package conductance, and hydraulic conductivity values of the main West Crane aquifer (Doherty, 2016; Doherty and Hunt, 2010).

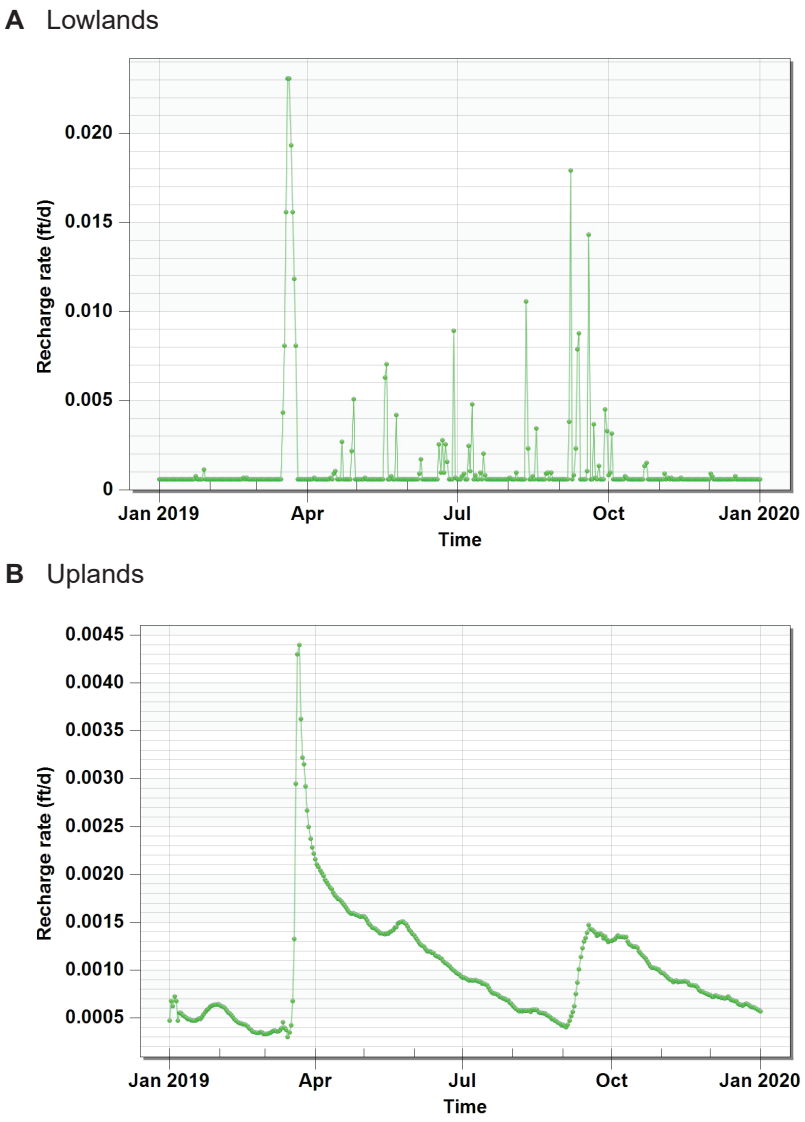

Figure 15. Lowland and upland recharge patterns applied in the groundwater models. The patterns are the same for each lowland and each upland polygon in the model, but the magnitude varies as driven by PEST.

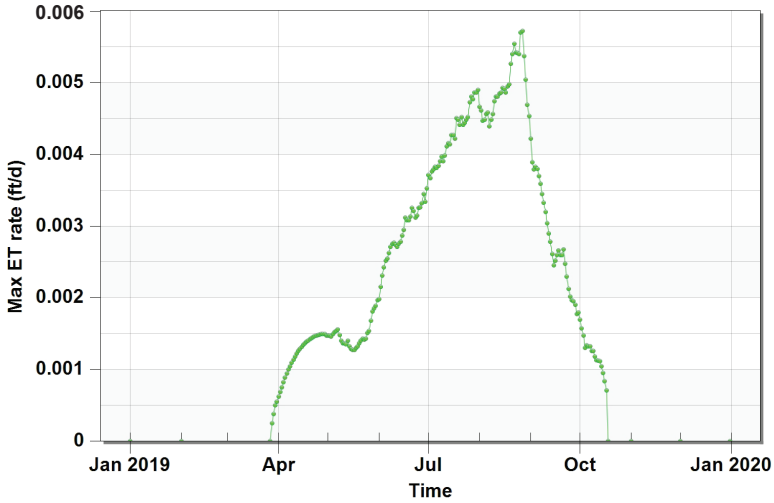

Figure 16. Maximum evapotranspiration (ET) rate pattern as applied in the 1-yr transient model version.

The final PEST calibration involved using the pilot-point method to refine the spatial distribution of hydraulic conductivity values (both horizontal hydraulic conductivity and vertical anisotropy ratio) for the West Crane aquifer in the overlying glacial till/fine-grained material, and the overlying alluvium of modern stream channels. The pilot-point method was also used to estimate S_s values in the confined West Crane aquifer and S_y values in the overlying unconfined glacial till/fine-grained materials and alluvial materials. The pilot-point method allows for estimation values of heterogenous hydraulic parameters spatially across a model grid with a lower computational effort than estimating values at each model grid cell (Doherty and others, 2010). Pilot points are discrete locations where parameter values are estimated, and those estimated values are distributed to individual model cells through spatial interpolation. For the West Crane aquifer, 169 pilot points were each spatially distributed for horizontal hydraulic conductivity, vertical hydraulic conductivity anisotropy ratio, and S_s. For the glacial till/fine-grained materials, 125 pilot points were each spatially distributed for horizontal hydraulic conductivity, vertical hydraulic conductivity anisotropy ratio, and S_y. For the stream alluvium, 19 pilot points were each spatially distributed for horizontal hydraulic conductivity, vertical hydraulic conductivity anisotropy ratio, and S_y. Additional horizontal hydraulic conductivity pilot points were added to the West Crane aquifer at the locations of aquifer testing (15 additional locations) and also in two areas where PEST HP was not initially able to match observed groundwater-level data (20 additional locations).

This additional calibration effort was performed using PEST HP (where "HP" stands for "high performance" or "highly parallelized" version of PEST) using 36 computing nodes with singular value decomposition (SVD) methods to speed the overall computing time (Doherty, 2021; Doherty and Hunt, 2010). Also, this calibration was performed on both the steady-state and transient model versions being considered simultaneously and cohesively, i.e., both versions used the same inputs other than the differences in simulated aquifer stresses of groundwater recharge and pumping.

Steady-State Calibration Results

Analysis of how well a model simulates observed conditions is based partially on statistics related to model residuals (the difference between simulated and observed groundwater levels). Standard calibration statistics include the average residual, absolute average residual, root mean squared error (RMSE, which gives greater weight to larger residuals), and the scaled RMSE (RMSE divided by the total range of measured groundwater levels, a measure of how well the model simulates groundwater flow gradients). Table 2 provides a summary of these statistics for the monitoring well locations in the West Crane aquifer steady-state model version.

Table 2. West Crane aquifer steady-state model version bulk calibration statistics.

Statistic	Value
Residual Mean (ft)	-0.15
Absolute Residual Mean (ft)	1.58
Residual Standard Deviation (ft)	1.86
RMSE (ft)	1.87
Minimum Residual (ft)	-4.23
Maximum Residual (ft)	3.44
Number of Observations	77
Range in Observations (ft)	164.5
Scaled Residual Standard Deviation	1.13%
Scaled Absolute Residual Mean	0.96%
Scaled RMSE	1.14%

It is important to note that no single set of statistical criteria exist that quantify a well-calibrated model, since modeling by necessity requires subjectivity and the calibration success is directly dependent on the modeling objective (Anderson and others, 2015). The slightly negative residual mean (-0.15 ft) indicates that on average, there is minimal bias where the model slightly overestimates heads (negative values indicate overestimation because each residual value is calculated as simulated value minus observed value), and the absolute residual mean suggests that the groundwater flow solution is typically within 1.58 ft of the observed values. Figure 17 is a scatter plot comparing the steady-state model version simulated and observed groundwater-level elevations, showing that the simulated elevations relative to the observed values generally fall near the 1:1 line and that the minimum and maximum residuals fall within ± 5 ft. The RMSE is 1.87 ft, and the scaled RMSE is only slightly greater than 1%, further indicating that the steady-state version is well-calibrated to the stresses and groundwater-level observation data.

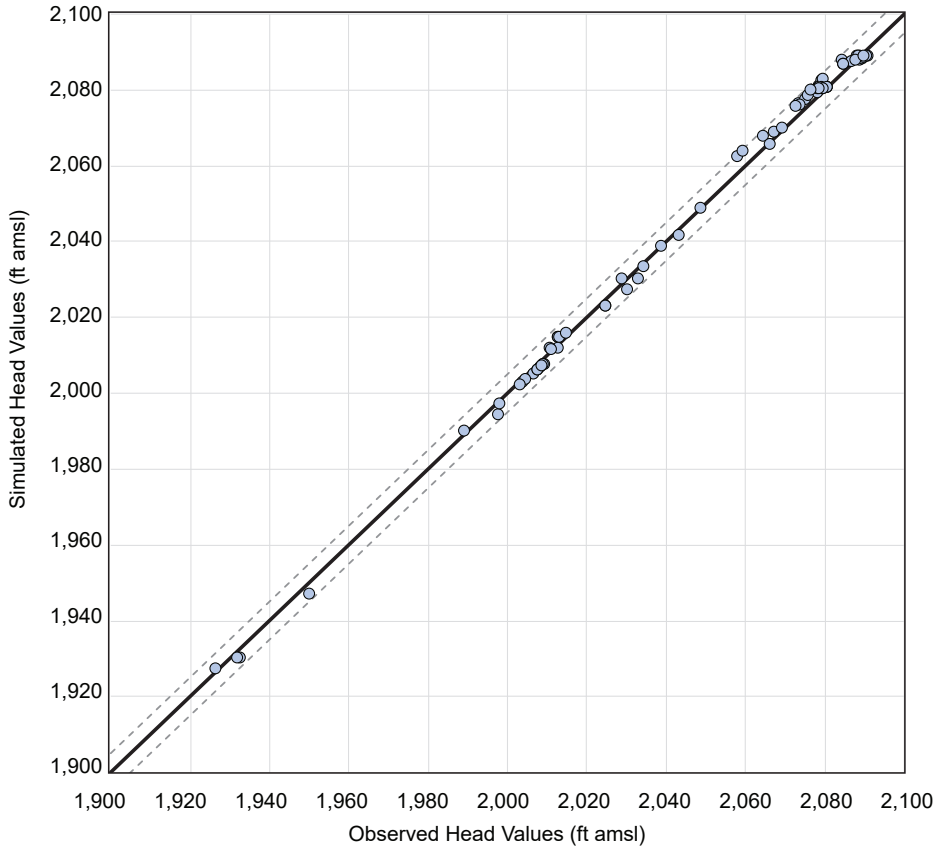

Figure 17. The steady-state model version calibration shows that all of the simulated head values at monitoring wells in the aquifer calibrated within ± 5 ft of the observed values (dashed lines).

The initial values assigned to the Drain Package cells in the steady-state model were based on estimated long-term stream baseflow discharges. The calibrated flow values agreed well with the target values (within about one percent; table 3). Water levels, recharge, discharge, and water use in the West Crane aquifer are in constant flux, and therefore the steady-state model version may be best used in the future as a tool for quickly evaluating long-term average changes in the aquifer related to potential different future management or climate regimes.

Table 3. Estimated observed versus computed (simulated) flow out drains in the steady-state model.

Drain Name	Estimated Observed Flow (average flow, ft^3/s)	Simulated Flow (model result, ft^3/s)
Crane Creek	1.3	1.5
Sears Creek	0.7	0.7
Garden Creek	0.1	0.1
Peabody Creek	0.1	0.1
Fox Creek	0.7	0.6

Transient Calibration Results

Table 4 summarizes the groundwater-level calibration statistics for the monitoring well locations in the West Crane aquifer transient model version. The slightly negative residual mean (-0.12 ft) indicates that there is minimal bias where the model slightly overes-

Table 4. West Crane aquifer transient model bulk calibration statistics

Statistic	Value
Residual Mean (ft)	-0.12
Absolute Residual Mean (ft)	1.69
Residual Standard Deviation (ft)	2.25
RMSE (ft)	2.25
Minimum Residual (ft)	-8.76
Maximum Residual (ft)	6.27
Number of Observations	19064
Range in Observations (ft)	160.61
Scaled Residual Standard Deviation	1.40%
Scaled Absolute Residual Mean	1.05%
Scaled RMSE	1.40%

timates heads (negative values indicate overestimation because each residual value is calculated as simulated value minus observed value). The absolute residual mean suggests that the groundwater flow solution is typically within 1.69 ft of the observed values. Figure 18 is a scatter plot comparing the simulated to observed groundwater heads; it shows that the simulated to the observed values fall near the 1:1 line, though some of the residuals are outside ± 5 ft. These outliers are primarily the result of observed recharge events that are not captured in the model recharge inputs. The transient model RMSE is 2.25 ft, and the scaled RMSE is approximately 1.4%, indicating that the model is overall well-calibrated to the 2019 transient model stresses and groundwater-level observation data.

Hydrographs comparing observed data to simulated data show the model reproduces groundwater-level changes in response to pumping stresses at representative wells (fig. 19). Site locations are shown in figures 6 and 7. The hydrograph for well 296815 captures the 2019 spring recharge event that is evident in the modeled and observed data. The effects of nearby irrigation wells are evident in the hydrographs for wells 283134, 253450, and 279891.

Simulated Groundwater Budget

Table 5 summarizes the 2019 transient model budget results with comparisons to the low and high conceptual water budget estimates (also previously presented in table 1). Overall, the simulated groundwater budget component values correspond reasonably with the conceptual estimated from field data and analytical calculations. The simulated recharge inputs are approximately 2.7 times greater than the low conceptual budget estimate. The simulated recharge is much less than the high conceptual budget estimate because the high conceptual estimate is based on different years with snowmelt and rainfall events that produced the highest groundwater-level responses for each event

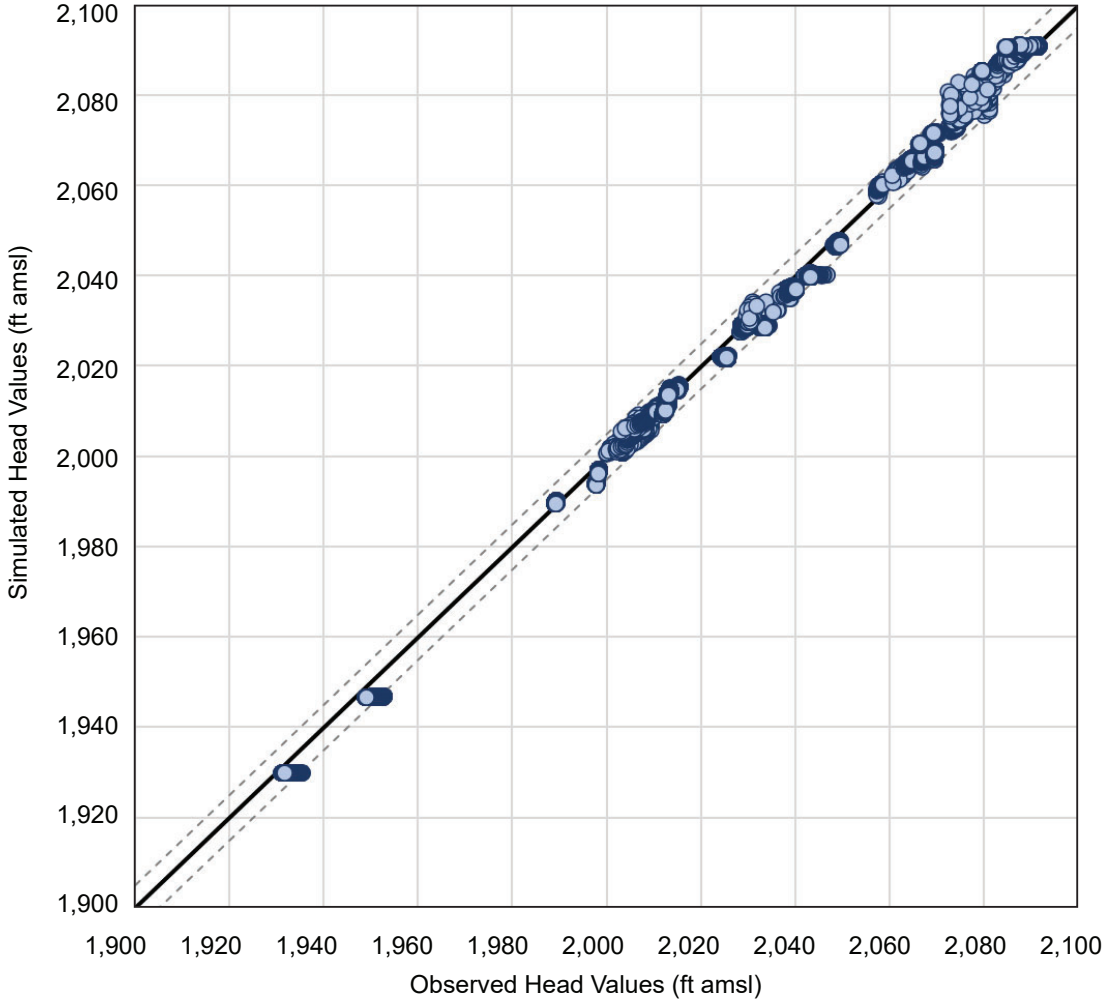

Figure 18. The transient model version calibration shows that the simulated head values at monitoring wells in the aquifer generally fit a 1:1 line, though some values are outside ± 5 ft of the observed values (dashed lines).

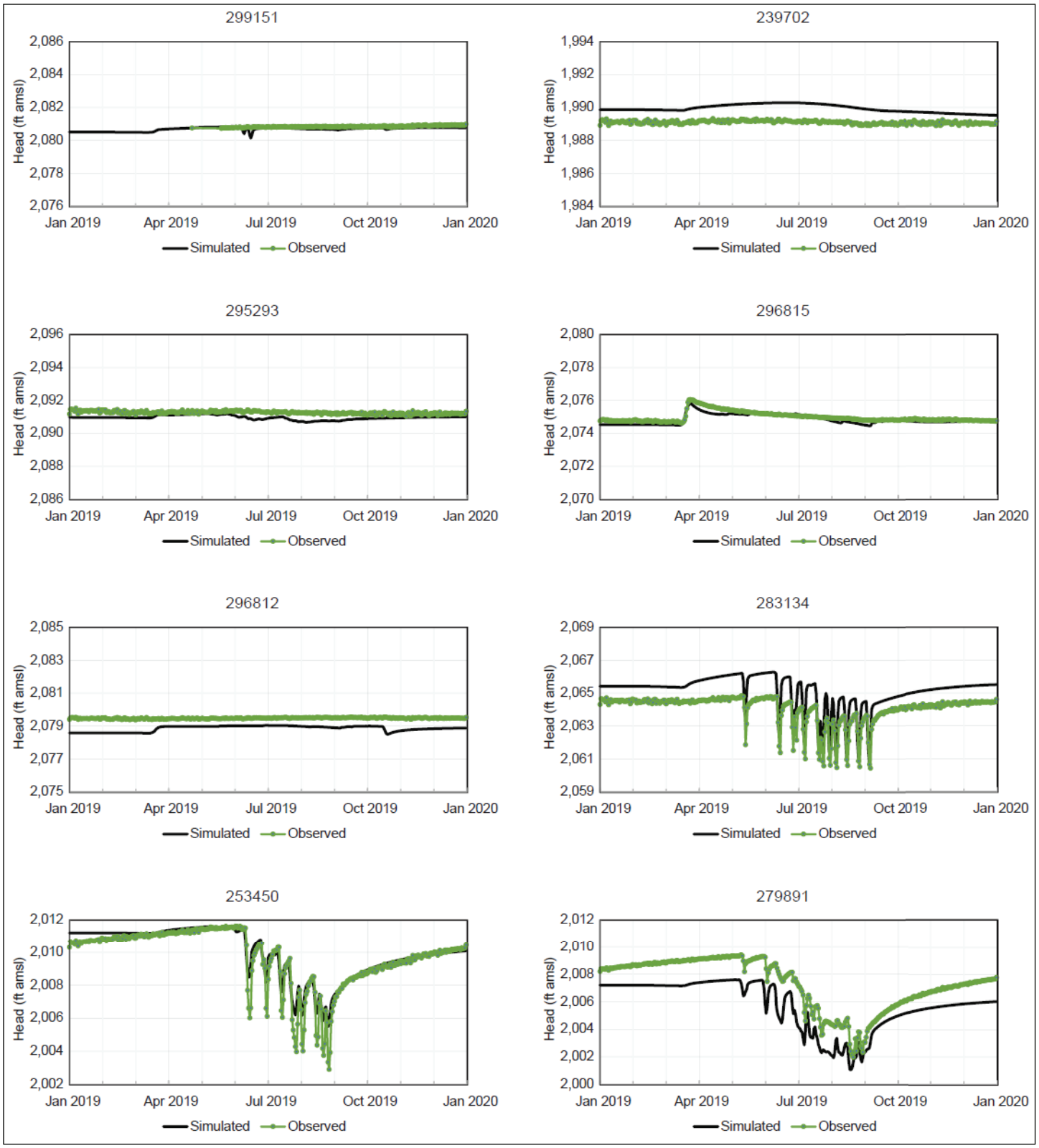

Figure 19. One-year transient model version calibration hydrograph results. Observed data (green dotted line in each graph) compared to simulated data (the black solid line in each graph). Graph locations are shown in figures 6 and 7. Notice the spring recharge event in late March 2019 at well 296815, and the pumping of nearby irrigation wells at 283134, 253450, and 279891.

Table 5. West Crane aquifer 2019 transient model simulated groundwater budget and conceptual budget.

Inflow			
Budget Component	Low Conceptual Estimate (acre-ft/yr)	High Conceptual Estimate (acre-ft/yr)	Simulated Value (acre-ft/yr)
Rainfall recharge	0	10,100	5,493[a]
Snowmelt recharge	2,020	30,300	
Total Inflow	2,020	40,400	5,493
Outflow			
Budget Component	Low Estimate (acre-ft/yr)	High Estimate (acre-ft/yr)	Simulated (acre-ft/yr)
ET	390	2,300	427
Net groundwater flow out at aquifer margins[b]	1,690	2,830	332
Streams	1,110	1,960	2,757
Pumping[c]	1,165	5,079	1,165
Total Outflow	4,355	12,169	4,681
Calculated Change in Aquifer Storage	-2,335	28,231	812

[a]Model-simulated recharge includes both rainfall and snowmelt recharge
[b]Groundwater flows in from and out of the aquifer margins presented as the net outflow.
[c]Low pumping estimate represents 2019 reported irrigation pumping volume and high estimate represents 2019 irrigation season appropriated volume.

type (2011 for snowmelt and 2014 for rainfall). The simulated irrigation well pumping is represented by a specified-flow boundary condition and exactly matches the low "estimate" for pumping because the 2019 irrigation actual pumping was used as the low value for the estimated water budget in table 1 as well as the model input pumping. The other model outflows (ET, net groundwater flow out, and discharge to streams) were simulated near the low conceptual budget estimate values. The simulated change in storage for the aquifer in 2019 was 812 acre-ft, approximately 15% of the model input recharge.

The simulated budget components outside the estimated conceptual low/high range were net groundwater flow and discharge to surface streams. Net groundwater flow out at the aquifer margins was simulated to be 332 acre-ft compared to a low estimate of 1,690 acre-ft and a high estimate of 2,830 acre-ft (table 5). The estimated net groundwater flow out of the aquifer was estimated using a Darcy flow-based approach, which introduces significant uncertainties owing to inherent simplifications of aquifer cross-sectional area, hydraulic gradient, and aquifer material hydraulic conductivity in those calculations. Discharge to streams was simulated to be 2,757 acre-ft in 2019 compared with a low estimate of 1,110 acre-ft and a high estimate of 1,960 acre-ft. The simulated discharge of 2,757 acre-ft/yr is equivalent to a stream discharge of 3.8 cfs, whereas the estimated value of 1,960 acre-ft/yr represents 2.7 cfs. The results indicate that overall, the apparent initial overestimate of net groundwater discharge from the West Crane aquifer margins was balanced by the initial underestimate of discharge to streams (table 5).

Sensitivity Analysis

The calibrated groundwater model was developed using available hydrogeologic data; PEST was used to adjust the input parameters to optimize the simulation results to the observed data. A simple sensitivity analysis was performed on the transient model version by multiplying and dividing the input parameters by factors of 1.5, 2, and 4 and comparing the resulting RMSE to that of the calibrated model. The parameters

tested were the hydraulic conductivity and storage coefficients for each stratigraphic unit (note that the modern stream alluvium and glacial till/fine-grained deposits were combined for this sensitivity exercise), recharge rate, DRN Package conductance, and maximum evapotranspiration rate. The model is most sensitive to changes in hydraulic conductivity in the West Crane aquifer and recharge. Figure 20 shows the changes in RMSE for the four parameter sets that exhibited more than 0.5 ft change in RMSE over the adjustment factors tested, hydraulic conductivity in the West Crane aquifer, recharge, hydraulic conductivity in the glacial till/fine-grained material and alluvium, and the vertical anisotropy of hydraulic conductivity in the glacial till/fine-grained material and alluvium. The calibration exhibited only marginal sensitivity to remaining input parameters in this exercise.

Model Scenarios

The transient model version was used to evaluate the water-level response related to changes in irrigation pumping (scenarios 1–3) and infiltrating water into gravel pits or other structures as managed aquifer recharge (MAR; scenario 4). Four different groundwater use scenarios were evaluated using the transient model for 2019 to assess the aquifer response. Scenario results were compared to the baseline 2019 model (table 6).

Scenario 1

The first scenario eliminated all irrigation pumping. This scenario resulted in a significant increase in groundwater storage, of approximately the same magnitude of the calculated volume of wells pumped in the baseline scenario. There was a minor increase in simulated stream discharge but relatively little impact to ET and groundwater flow (table 6, fig. 21).

Scenario 2

For the second scenario, well 305427 (drilled in fall 2019 and not pumped during the irrigation season in the baseline model) was pumped at its maximum permitted allocation of 314 acre-ft during the irrigation season (table 7). This additional pumping was predominantly balanced by decreases in the amount of water going into storage, with only minor changes to other water budget components (table 6, fig. 21).

Scenario 3

The third scenario involved increasing the withdrawals to the maximum permitted amount for each well (table 7). As discussed earlier, the reported

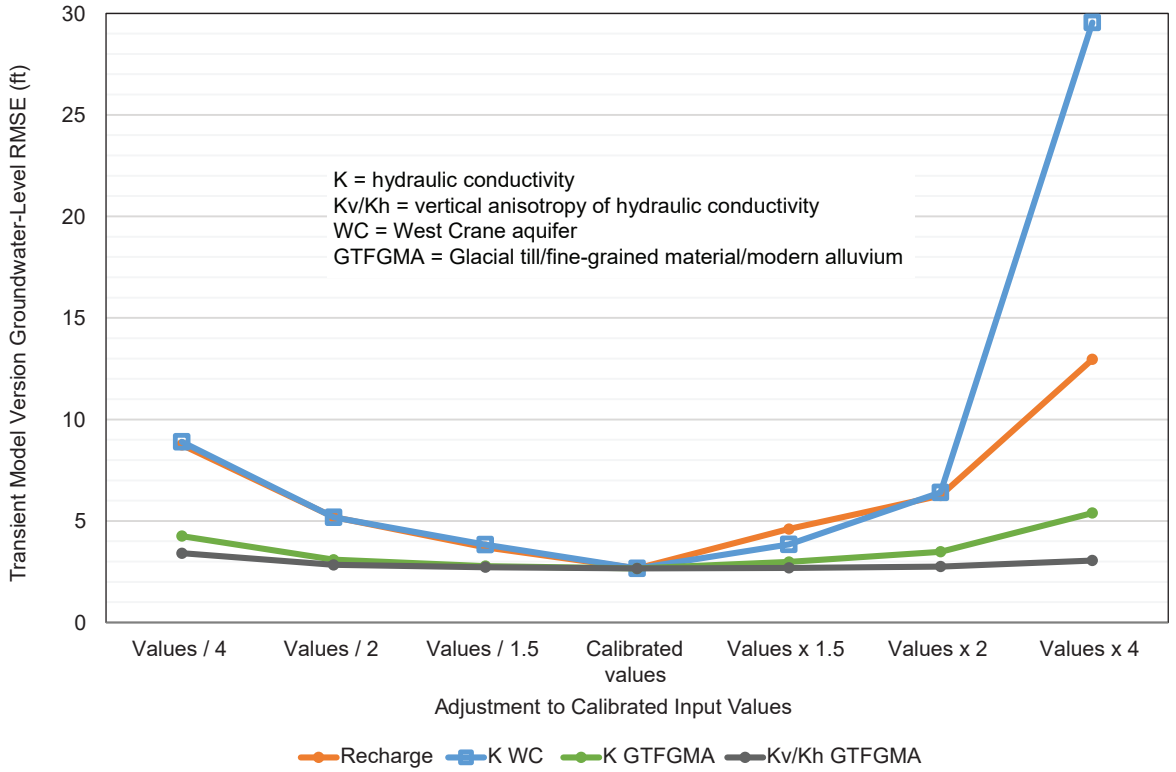

Figure 20. Model input parameter sensitivity analysis results for those parameters that were determined to be not insensitive. Hydraulic conductivity in the West Crane aquifer and recharge are the most sensitive parameters.

Table 6. Scenario simulated groundwater budget results (acre-ft) for the baseline model and four scenarios. Groundwater in and out was calculated at the aquifer margins.

Scenario	Description	Recharge in	Groundwater in	ET out	Groundwater out	Discharge to Surface Water out	Well Pumping out	Net Storage Change
Baseline	Transient 2019 1-yr model	5,493	1,128	427	1,461	2,757	1,165	812
Scenario 1	No well pumping	5,493	1,126	428	1,461	2,895	0	1,834
Scenario 2	Add well 305427 pumping at maximum allocation	5,493	1,129	427	1,460	2,750	1,479	507
Scenario 3	All irrigation wells pumping at maximum allocation (including well 305427)	5,493	1,145	423	1,455	2,359	5,078	-2,676
Scenario 4	MAR of excess surface water flow	5,956	1,072	427	1,475	2,881	1,165	1,080

Table 7. Pumping well volumes in the 1-yr transient baseline model and at maximum appropriation scenarios.

GWIC ID	Name in Models	Baseline Model (2019 Pumping Volumes, acre-ft)	Scenario 3 (Full Appropriation Volumes, acre-ft)
249505	249505 KJ1	96	310.5
250211	Wyman 1	149.4	342.4
253448	253448 Bradley 1	98.4	272.5
284325	284325 KJ2	133.7	310.5
285476	285476 CJ2	149.6	386
285659	285659 CJ1	149.6	386
290760	290760 DJorg1	139.2	375
291010	291010 CJ3	149.6	386
295397	Ler 1	14.4	362
296426	Lange 1	66.2	400
296536	Basta 1	0	66
296537	296537 Bast1	0	66
296761	296761 Basta 1-3	0	66
300586	Lange 2	0	325.3
303552	303552 Jjorg1	18.8	710.1
305427	305427[1]	0	314.4

[1]Appears in both Scenarios 2 and 3.

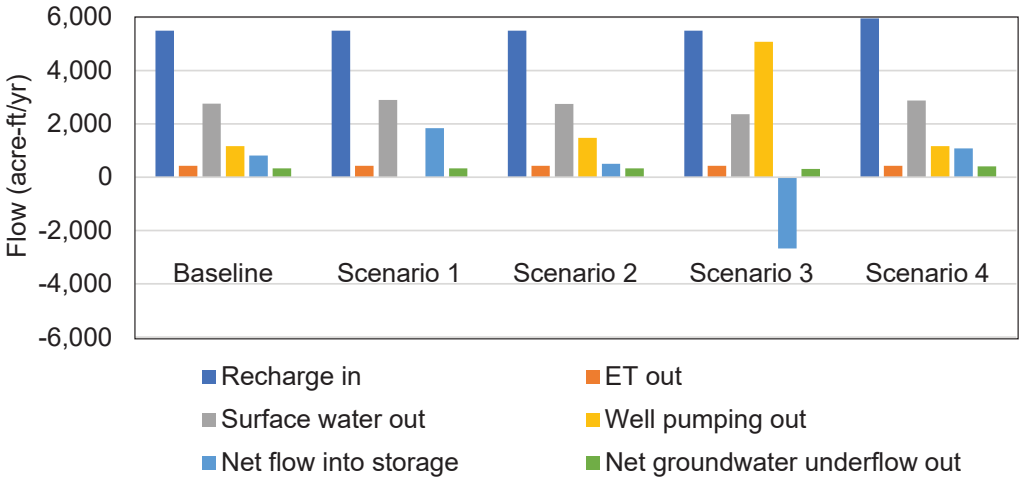

Figure 21. Chart showing water inputs and outputs for the baseline model and four scenarios.

volume pumped by irrigators was approximately a quarter of the permitted volume for 2019. The higher simulated pumping rates resulted in simulated decreases in groundwater storage as stored water became the primary source of increased irrigation withdrawals. The simulated decrease in streamflow out of the model was approximately 14% of the baseline model result, while changes to the remaining water budget components were minimal (table 6, fig. 21).

Scenario 4

The fourth scenario simulated a hypothetical MAR project by infiltrating 463 acre-ft of water into gravel pits or other potential infiltration structures as managed aquifer recharge. The dry creek bottoms, where creeks cross the aquifer, have ample exposed gravel and are convenient sites for gravel pit operations. Once the gravel has been mined, large depressions remain. This scenario simulates approximately 20 acres of pits in each of four drainages: Crane Creek, Sears Creek, Dunlap Creek, and Garden Coulee. The pits are assumed to fill with runoff water and leak 20 acre-ft/d for 6 days. This leakage was simulated using 21 injection wells in each drainage, one per model cell in likely areas for gravel pits. This simulation was accomplished by using a second Recharge package (using the multiple boundary condition package capability of MODFLOW 6) to simulate recharge at 84 model cells in clusters of 21 model cells each along four separate drainages: Crane Creek, Sears Creek, Dunlap Creek, and Garden Coulee (fig. 22; Langevin and others, 2017). The infiltrated water was applied at a constant rate for 6 days, March 17 through March 22, 2019.

Of the 463 acre-ft of additional recharge, the model simulated that approximately 58% flowed into groundwater storage and 27% was discharged to surface streams (table 6, fig. 21). Changes to the simulated net groundwater flow out of the model domain accounted for the remaining 15% of the additional recharge. The change in the simulated net groundwater flow out of the model domain at the aquifer margins occurs because the additional recharge results in slight changes to the simulated hydraulic gradients such that the upstream gradients are shallower (resulting in less groundwater inflow, 12% of the additional recharge) and downstream gradients are steeper (resulting in more groundwater outflow, 3% of the additional recharge). The impact on simulated ET was minimal (less than 1% of the additional recharge).

These scenarios show that groundwater withdrawals and additions to the aquifer are balanced mostly by changes in groundwater storage.

MODEL LIMITATIONS AND RECOMMENDATIONS

The transient model is based on data from 2019, which had an unusually wet September. For evaluating future uses, it could be used as is, with a recognition that the recharge modeled in September is inflated, and so results will likely be somewhat different for a year with a more average or below average precipitation pattern. Two other options are (1) reduce September recharge amounts to more typical amounts, or (2) build the 1-yr input data using average precipitation and snowmelt data instead of any specific year. For these options, the transient model input can be repeated annually. Then, long-term effects of pumping and recovery for multiple years could be evaluated assuming repetition of these annual aquifer stress conditions.

The transient model also could be updated using more recent precipitation and pumping data. Recharge volumes were developed through episodic master regression and adjustments driven by initial PEST simulations. Summer precipitation varies widely based on the geographic spacing of storm cells. Additional climate stations over the aquifer and watersheds that supply recharge could provide better recharge estimates. Winter precipitation typically recharges the aquifer during spring runoff. Developing better methods of estimating the effective snowpack would also provide better estimates of recharge from spring runoff. A watershed-scale soil–water balance modeling approach with the USGS Soil–Water Balance 2 model (or similar tool) may provide better estimates of snowmelt- and precipitation-based net infiltration and groundwater recharge (Westenbroek and others, 2018).

Any future calibration efforts should focus on horizontal hydraulic conductivity values and recharge, including potentially adding recharge parameters to PEST simulations. The current model calibration reflects an effort to simultaneously calibrate both the March 2018 steady-state and the 1-yr 2019 transient model versions with the same aquifer parameter input values but with different aquifer stresses and observa-

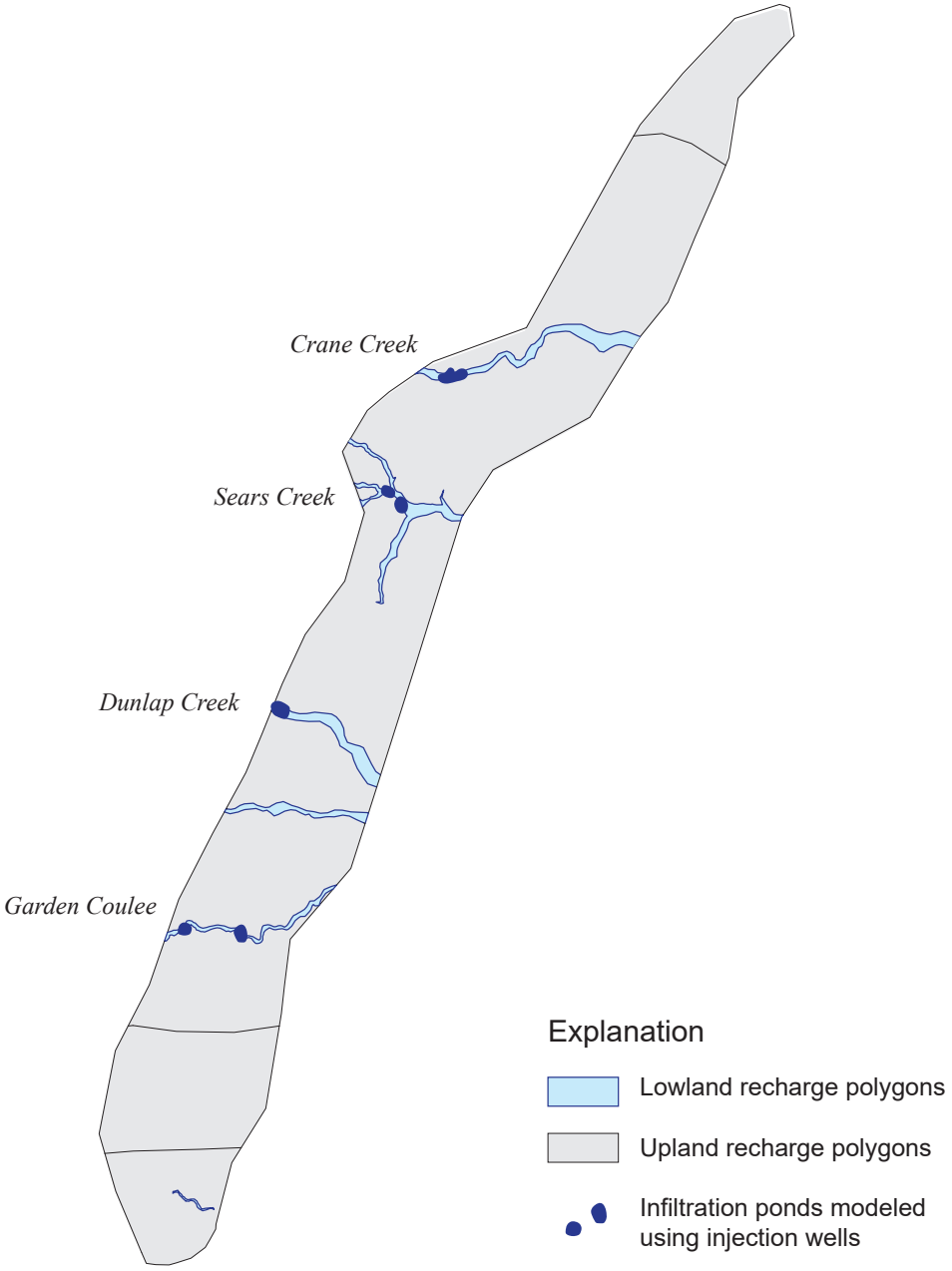

Figure 22. Placement of infiltration ponds in the MAR scenario. Infiltration ponds were simulated by placing injection wells in each of four drainages: Crane Creek, Sears Creek, Dunlap Creek, and Garden Coulee.

tion data, and as such is a compromise. While both versions have potential value for performing predictive analyses, it is recommended that future calibrations use only the transient construct. The resulting updated model input parameter values could then be applied in the steady-state model followed by adjustments to the assumed (and highly uncertain) steady-state recharge rates.

One additional consideration is that distances between irrigation pumping wells and monitoring wells cannot be replicated with the current 200-ft grid spacing since many of the monitoring wells are less than 200 ft from the pumping wells. Using an unstructured model grid in MODFLOW 6 with smaller grid spacing in the vicinities of irrigation pumping wells would likely provide improved simulation of the cones of depression around pumping wells.

CONCLUSIONS

The objective of the study was to evaluate the extent and groundwater availability of the West Crane aquifer. Reiten and Chandler (2023) identified the West Crane aquifer as a buried valley that extends for about 22 mi and is parallel to the Yellowstone River. The aquifer is about 1 mi wide and up to 300 ft deep. The numerical groundwater flow model presented in

this report was developed from the data and interpretations included in Reiten and Chandler (2023). The model provides a structure to mathematically simulate groundwater flowing to, through, and from the West Crane aquifer. The model accounts for the overall lateral and vertical geometry of the aquifer, and the calibrated input hydraulic conductivity and storage parameters provide a framework for simulating the availability of groundwater in specific local areas as well as throughout the aquifer. The model files are available for download through the MBMG publication page (https://doi.org/10.59691/OZVN9020) and can be used by area water managers to simulate impacts from increased water use through pumping, aquifer response to climatic changes, the potential impacts of MAR projects, or other management strategies.

The steady-state model version was built using average annual data, and is useful for future applications with little modification. The model can be modified to evaluate long-term pumping impacts or changes in climate conditions.

The 1-yr transient model version was constructed and calibrated using 2019 data related to aquifer stresses (i.e., groundwater recharge and pumping) and groundwater-level data. The model results refined our understanding of the groundwater budget and the magnitude and distribution of recharge and discharge from the aquifer. The model-simulated 2019 groundwater budget compared more closely to the lower estimates of the conceptual groundwater recharge for the aquifer because the higher conceptual estimates of recharge may represent a relatively uncommon combination of snowmelt and rainfall events (tables 1, 5). The 2019 budget also indicated less groundwater flow out of the aquifer and greater groundwater discharge to streams than the conceptual water budget. Wet years that result in greater groundwater recharge would likely show increased groundwater flow out, stream discharge, and ET, as well as increased storage in the aquifer.

The first three predictive scenario models also illustrate the ability to utilize this aquifer as a source of water for agricultural irrigation with only minor impacts to surface-water discharges and minimal impacts to ET. The fourth predictive scenario model indicates that a surface infiltration MAR project would primarily increase groundwater stored in the aquifer but would also secondarily drive some increased discharge from the aquifer to streams.

Suggestions for future model scenarios include decreasing the September recharge inputs to more typical values, or structuring the recharge to reflect average conditions for all months. The transient model could also be extended further in time using post-2019 (or even pre-2019) groundwater withdrawal and water-level data. Future calibration efforts should focus on the hydraulic conductivity values and recharge as these parameters were found to have the greatest effect on overall model results.

ACKNOWLEDGMENTS

Landowners and farmers along the entire aquifer from Fox Creek to Burns Creek have been very helpful and supportive of this groundwater research. They have allowed access for test drilling, monitor well installation, flume installation, and continuous monitoring. Without this collaboration, the project would not have been possible. Current and past Montana Bureau of Mines and Geology staff contributed to mapping and well inventories of this area through the Statemap program (Susan Vuke) and Ground Water Characterization Program (Larry Smith and John LaFave). Simon Bierbach assisted with data analysis, figure development, and GIS mapping. Kirk Waren assisted in assembling this model report, and adding a few short narratives in places.

The Richland County Conservation District was the project sponsor. Their interest and support drove the project from the start. In particular they provided contact information for the producers, field technicians, and data loggers used to monitor aquifer water-level fluctuations.

REFERENCES

Anderson, M.P., Woessner, W.W., and Hunt, R.J., 2015, Applied groundwater modeling: Simulation of flow and advective transport: San Diego, Calif., Academic Press, 564 p.

Aquaveo, LLC, 2009, Groundwater modeling system (GMS), v. 7.0.

Aquaveo, 2019, GMS User manual 10.4: Salt Lake City, UT, available at https://www.xmswiki.com/wiki/GMS:GMS_User_Manual_10.4 [Accessed 8/20/2022]

Batu, V., 1998, *Aquifer hydraulics: A comprehensive guide to hydrogeologic data analysis*: New York, John Wiley & Sons, 727 p.

Chandler, K., and Reiten, J., 2020, West Crane buried valley aquifer: A hidden resource: Montana Bureau of Mines and Geology Information Pamphlet 13, 4 p.

Doherty, J.E., 2016, PEST model-independent parameter estimation user manual part I: PEST, SENSAN and Global Optimisers (6th ed): Watermark Numerical Computing, 369 p.

Doherty, J.E., 2021, PEST_HP—PEST for highly parallelized computing environments: Watermark Numerical Computing, 90 p.

Doherty, J.E., and Hunt, R.J., 2010, Approaches to highly parameterized inversion—A guide to using PEST for groundwater-model calibration: U.S. Geological Survey Scientific Investigations Report 2010–5169, 59 p.

Doherty, J.E., Fienen, M.N., and Hunt, R.J., 2010, Approaches to highly parameterized inversion: Pilot-point theory, guidelines, and research directions: U.S. Geological Survey Scientific Investigations Report 2010–5168, 36 p.

Duffield, G., 2007, AQTESOLV for Windows ver. 4.5 user's guide, available from https://www.aqtesolv.com [Accessed March 2023].

Environmental Simulations Inc. (ESI), 2020, Guide to using Groundwater Vistas Version 8, 523 p.

Harbaugh, A.W., 2005, MODFLOW-2005, the U.S. Geological Survey modular ground-water model— The ground-water flow process: U.S. Geological Survey Techniques and Methods 6-A16, available at https://pubs.usgs.gov/tm/2005/tm6A16/ [Accessed May 2025].

Harbaugh, A.W., Banta, E.R., Hill, M.C., and McDonald, M.G., 2000, MODFLOW-2000, the U.S. Geological Survey modular ground-water model—User guide to modularization concepts and ground-water flow process: U.S. Geological Survey Open-File Report 00-92, 121 p.

Heath, R.C., 1983, Basic ground-water hydrology: U.S. Geological Survey Water-Supply Paper 2220, 86 p.

Langevin, C.D., Hughes, J.D., Banta, E.R., Provost, A.M., Niswonger, R.G., and Panday, Sorab, 2017, MODFLOW 6 modular hydrologic model: U.S. Geological Survey Software, https://doi.org/10.5066/F76Q1VQV

Miller, K.G., Norbeck, P., and Reiten, J.C., 1998, Montana source water protection: Technical guidance manual, parts 1 and 2: Montana Bureau of Mines and Geology Open-File Report 378, 281 p.

Nimmo, J.R., and Perkins, K.S., 2018, Episodic master regression evaluation of groundwater and streamflow hydrographs for water-resource estimation: Vadose Zone Journal, v. 17, no. 1, p. 1–25, https://doi.org/10.2136/vzj2018.03.0050

Reiten, J., and Chandler, K., 2013, Extent and hydrogeology of the lower Yellowstone buried aquifer system, Richland County, Montana: Abstract to the Midwest Groundwater Conference, September 2013, Bismarck, ND.

Reiten, J., and Chandler, K., 2014, Extent and hydrogeology of the lower Yellowstone buried channel aquifer system, Richland County, Montana: Abstract to the Geological Society of America Rocky Mountain (66th annual) and Cordilleran (110th annual) joint meeting, May 2014, Bozeman, Mont.

Reiten, J., and Chandler, K., 2019, A tale of two aquifers: A study in aquifer sustainability: Abstract to the MT AWRA Conference, Red Lodge, Mont.

Reiten, J., and Chandler, K., 2021, West Crane aquifer test summaries, Richland County, Montana: Montana Bureau of Mines and Geology Open-File Report 737, 62 p., available at https://www.mbmg.mtech.edu/mbmgcat/public/ListCitation.asp?pub_id=32344 [Accessed May 2025].

Reiten, J., and Chandler, K., 2023, Hydrogeology and irrigation potential of the West Crane aquifer, Richland County, Montana: Montana Bureau of Mines and Geology Open-File Report 760, 44 p., 3 sheets, https://doi.org/10.59691/AKZS9766

Smith, L.N., 1998, Thickness of unconsolidated deposits, Lower Yellowstone River Area: Dawson, Fallon, Prairie, Richland, and Wibaux Counties, Montana. Part A. Descriptive overview and basic data: Montana Bureau of Mines and Geology Ground-Water Assessment Atlas 1-A, 43 p., available at https://www.mbmg.mtech.edu/mbmgcat/public/ListCitation.asp?pub_id=10298 [Accessed May 2025].

Westenbroek, S.M., Engott, J.A., Kelson, V.A., and Hunt, R.J., 2018, SWB Version 2.0—A soil-water-balance code for estimating net infiltration and other water-budget components: U.S. Geological Survey Techniques and Methods, book 6, chap. A59, 118 p., https://doi.org/10.3133/tm6A59

Woessner, W.W., and Poeter, E.P., 2020, Hydrogeologic properties of earth materials and principles of groundwater flow: Groundwater Project, Guelph, Ontario, Canada, 205 p., available at https://gw-project.org/books/hydrogeologic-properties-of-earth-materials-and-principles-of-groundwater-flow/ [Accessed May 2025].

WRCC, 2021, Western Regional Climate Center: Retrieved from Climate Data, available at http://wrcc.dri.efu/cgi-bin/cliMAIN.pl?;mt7382 [Accessed January 2021].